Toxoplasma gondii co-opts the unfolded protein response to enhance migration and dissemination of infected host cells

Leonardo Augusto[a,b], Jennifer Martynowicz[c], Parth H. Amin[a], Nada S. Alakhras[a], Mark H. Kaplan[c], Ronald C. Wek[a*], William J. Sullivan, Jr[b,c*]

[a]Department of Biochemistry & Molecular Biology, Indiana University School of Medicine, Indianapolis, Indiana, 46202.

[b]Department of Pharmacology & Toxicology, Indiana University School of Medicine, Indianapolis, Indiana, 46202.

[c]Department of Microbiology & Immunology, Indiana University School of Medicine, Indianapolis, Indiana, 46202.

Running title: *Toxoplasma* infection induces host UPR and migration

*Corresponding authors:

Ronald C. Wek
Showalter Professor
Indiana University School of Medicine
635 Barnhill Drive
MS 4067A
Indianapolis, IN 46202
(317) 274-0549; rwek@iu.edu

William J. Sullivan, Jr.
Showalter Professor
Indiana University School of Medicine
635 Barnhill Drive
MS A418C
Indianapolis, IN 46202
(317) 274-1573; wjsulliv@iu.edu

Abstract

Toxoplasma gondii is an intracellular parasite that reconfigures its host cell to promote pathogenesis. One consequence of *Toxoplasma* parasitism is increased migratory activity of host cells, which facilitates dissemination. Here we show that *Toxoplasma* triggers the unfolded protein response (UPR) in host cells through calcium release from the endoplasmic reticulum (ER). We further found that host IRE1, an ER stress sensor protein activated during *Toxoplasma* infection, also plays a noncanonical role in actin remodeling by binding filamin A in infected cells. By inducing cytoskeletal remodeling via IRE1 oligomerization in host cells, *Toxoplasma* enhances host cell migration *in vitro* and dissemination of the parasite to host organs *in vivo*. Our study identifies novel mechanisms used by *Toxoplasma* to induce dissemination of infected cells, providing new insights into strategies for treatment of toxoplasmosis.

Keywords: *Toxoplasma*, parasites, UPR, IRE1, PERK, cell migration, filamin A, host-pathogen interactions

Importance

Cells that are infected with the parasite *Toxoplasma gondii* exhibit heightened migratory activity, which facilitates dissemination of the infection throughout the body. In this study, we identify a new mechanism used by *Toxoplasma* to hijack its host cell and increase its mobility. We further show that the ability of *Toxoplasma* to increase host cell migration does not involve the enzymatic activity of IRE1, but rather IRE1 engagement with actin cytoskeletal remodeling. Depletion of IRE1 from infected host cells reduces their migration in vitro and significantly hinders dissemination of *Toxoplasma* in vivo. Our findings reveal a new mechanism underlying host-pathogen interactions, demonstrating how host cells are co-opted to spread a persistent infection around the body.

Introduction

Toxoplasma gondii is an obligate intracellular parasite capable of infecting any nucleated cell in warm-blooded vertebrates. Recent studies have revealed a striking degree of host cell remodeling taking place in *Toxoplasma*-infected cells that serves to facilitate pathogenesis and transmission. In addition to secreted parasite effectors that modulate host cell gene expression, *Toxoplasma* infection can alter immune responses and enable dissemination to other host tissues [1]. Therein, *Toxoplasma* can differentiate from the replicative tachyzoites to the latent bradyzoite stage, enabling formation of tissue cysts that persist for the lifetime of the infected host [2].

Upon host cell invasion, *Toxoplasma* forms a parasitophorous vacuole (PV) that serves as a protective niche that can interface with the host cell cytoplasm to sequester nutrients [3]. Curiously, *Toxoplasma* recruits the host endoplasmic reticulum (ER) to the PV via association between their respective membranes, although the reasons for this high affinity interaction are not yet understood [4, 5].

The ER is sensitive to the perturbations in protein homeostasis through a stress-sensing pathway known as the unfolded protein response (UPR). Three ER transmembrane proteins, IRE1, ATF6, and PERK operate as sensors that activate the UPR, leading to changes in gene expression that restore and expand the processing capacity of the organelle [6-8]. IRE1 (ERN1) is a protein kinase and endoribonuclease that facilitates cytosolic splicing of *XBP1* (XBP1s) mRNA, thereby enhancing expression of the XBP1s isoform, which induces transcription of genes involved in ER-associated protein degradation (ERAD), lipid synthesis, and protein folding [7, 8]. In response to ER stress, ATF6 transits from the ER to the Golgi apparatus where it is cleaved, releasing an N-terminal cytosolic fragment (ATF6-N) that enters the nucleus and

activates UPR-target genes involved in protein folding and transport [6, 9]. PERK (EIF2AK3) is the third UPR sensor, which phosphorylates eIF2α to direct translational and transcriptional modes of gene expression that regulate ER processing of proteins, metabolism, and the oxidation status of cells [6, 10]. While the three ER stress sensory proteins function in parallel, there is cross-regulation that serves to coordinate the timing and magnitude of the UPR. For example, PERK was reported to induce expression of RPAP2, which serves to dephosphorylate and repress IRE1, thereby providing a means for the cell to abort failed ER-stress adaptation and trigger apoptosis [11].

In addition to its role in the UPR, IRE1 was recently shown to modulate cytoskeletal remodeling and cell migration through direct interactions with the actin crosslinking factor filamin A [12]. The role of IRE1 in cytoskeletal remodeling is enhanced by pharmacological induction of ER stress, but occurs independent of IRE1 protein kinase and endoribonuclease activities [12]; rather, IRE1 serves as a scaffolding protein for filamin A to orchestrate changes in cellular motility. This is noteworthy because *Toxoplasma* stimulates host cell migration, turning its host cell into a "Trojan Horse" that can ferry parasites throughout the body [13]. Given the recruitment of host ER to the PV, we postulated that migratory activities mediated by IRE1 function in parasite dissemination. In the present study, we uncover a new mechanism by which *Toxoplasma* alters host ER homeostasis to produce hypermigratory activity in infected host cells. We show that during the course of *Toxoplasma* infection, the three UPR sensory proteins in the host cells are activated by a process involving calcium release from the ER, leading to IRE1 oligomerization, association with filamin A, and enhanced cell migration. Importantly, the IRE1-associated migration is a crucial determinant for successful dissemination of toxoplasmosis in a mouse model of infection.

Results

Induction of the UPR in *Toxoplasma*-infected host cells

It is currently unclear why intracellular tachyzoites recruit host ER to the parasite PV. To address whether *Toxoplasma* perturbs host ER homeostasis, we infected mouse embryonic fibroblast (MEF) cells with RH strain parasites and measured three primary markers of the host UPR over a 36-hour time course. Within 12 h of infection, *Toxoplasma* increased activation of PERK as measured by its self-phosphorylation (PERK-P), induced expression of ATF6 and formation of its cleavage product ATF6-N, and increased levels of the IRE1-derived spliced variant of XBP1 (XBP1s) **(Fig. 1A)**. It is noteworthy that whereas expression of ATF6-N and XBP1s were transient, with increased amounts of the proteins appearing between 12 to 20 h post-infection (hpi), PERK-P increased throughout the 36 h of infection **(Fig. 1A)**. These results indicate that *Toxoplasma* infection causes ER stress that activates each of the sensory proteins of the UPR with some differences in the duration of their induction.

Activation of IRE1 involves oligomerization that can be visualized by a pattern of punctate spots by IFA [14-16]. We expressed EGFP-tagged IRE1 in MEF cells that were deleted for the endogenous *IRE1* gene by CRISPR/Cas9 genome editing **(Fig. S1A-C)**; upon *Toxoplasma* infection, we observed formation of IRE1 foci that is consistent with reported IRE1 activation by oligomerization **(Fig. 1B)** [15, 16]. Furthermore, expression of *XBP1s* mRNA, and its downstream target genes involved in ERAD and protein folding, were induced upon *Toxoplasma* infection of wild-type (WT) MEF cells **(Fig. 1C)**. These results indicate that IRE1 activation and signaling occur in response to *Toxoplasma* infection.

To further study the timing of UPR induction and potential cross-regulation between the UPR sensors in infected cells, we measured *XBP1s* mRNA levels by RT-qPCR in WT, *IRE1*$^{-/-}$,

or *PERK*$^{-/-}$ MEF cells. In WT cells, levels of *XBP1s* mRNA rose sharply until 18 hpi **(Fig. 1D)**, consistent with the increase in XBP1s protein **(Fig. 1A)**. As expected, *XBP1s* mRNA was not detected in infected *IRE1*$^{-/-}$ cells **(Fig. 1D)**. By comparison, there was induced *XBP1s* mRNA that was sustained during 36 h of *Toxoplasma* infection in *PERK*$^{-/-}$ cells, indicating that without PERK, IRE1 continues to facilitate *XBP1s* expression **(Fig. 1D)**. These results are consistent with the idea that PERK governs IRE1 activity as previously reported [11] and suggests that in infected WT cells, PERK operates to attenuate the response of IRE1 after 18 hpi.

IRE1 affects calcium release from ER in *Toxoplasma*-infected cells.

Protein folding in the ER is highly sensitive to the concentration of calcium, which is released from the organelle by ryanodine receptors (RyR) and inositol 1,4,5-triphosphate (IP3)-receptors (IP_3R) [17]. The ER is a major reservoir of calcium; disruptions of calcium homeostasis can lead to unfolded proteins and initiation of the UPR [17]. To determine whether calcium content is altered in the host ER during *Toxoplasma* infection, we first measured cytosolic calcium in infected MEF cells. Over an 18-hour period, *Toxoplasma* infection induced a steady increase in host cell cytosolic calcium levels **(Fig. 2A, Fig. S2A)**. Basal calcium levels in the cytosol of *IRE1*$^{-/-}$ cells were lower compared to WT cells, as previously reported [18], with some increase upon parasite infection **(Fig. 2A, Fig. S2A)**. To assess the mode of calcium release from the host ER during infection, we monitored calcium transport using Fluo-4AM in the presence of antagonists of RyR or IP_3R. The cytosolic calcium levels were lower in infected cells treated with either antagonist, with the most robust calcium reduction occurring with inhibition of IP_3R **(Fig. 2B)**. We further addressed the contribution of RyR and IP_3R to calcium release by adding increasing doses of caffeine and IP_3, agonists of RyR and IP_3R receptor

activity [19], respectively, to WT and *IRE1*$^{-/-}$ cells infected with *Toxoplasma* for 18 h and incubated with Mag-Fluo-4. To compare calcium release between RyR and IP_3R in WT and *IRE1*$^{-/-}$ cells, the fluorescence values were represented as the percentage of calcium release and the respective start points were normalized to untreated WT and *IRE1*$^{-/-}$ cells, respectively. The RyR agonist enhanced calcium to similar levels in infected WT or *IRE1*$^{-/-}$ cells **(Fig. 2C)**. By comparison, the agonist IP_3 induced appreciable calcium release only in infected WT cells **(Fig. 2D)**, indicating a role for IRE1 in regulating IP_3R activity as previous reported [18]. Surprisingly, the percentage of calcium release was higher when IP_3R was stimulated compared to RyR, demonstrating that *Toxoplasma* infection differentially alters RyR and IP_3R activities. Collectively, these results suggest that *Toxoplasma* infection induces significant calcium release from the host ER by processes involving both IP_3R and RyR; this calcium release is influenced by IRE1 and is a likely contributor to the activation of the host ER-stress sensor proteins seen in Figure 1A.

IRE1 activation induces cell migration in infected cells

Toxoplasma triggers rapid morphological changes in host cells, including disappearance of podosome structures and appearance of lamellipodia [20]. IRE1 has recently been shown to have noncanonical functions in actin cytoskeletal remodeling by directly binding to filamin A [12]. To address whether activation of IRE1 by *Toxoplasma* infection enhances host cell migration, we quantified the number of lamellipodia per infected cell normalized to uninfected cells **(Fig. 3A, Fig. S3A)**. At 18 hpi, *Toxoplasma* infection increased the number of lamellipodia in WT cells and these structures were significantly diminished in IRE1-deficient cells **(Fig. 3A)**. By comparison, there were greater numbers of lamellipodia in PERK-deficient cells or those

166 treated with a PERK inhibitor, consistent with the idea that PERK is a negative regulator of IRE1
167 **(Fig. 3A)**. Of interest, treatment with inhibitors of IRE1, namely 4μ8c, which interferes with
168 endoribonuclease activity, and KIRA6, which blocks IRE1 protein kinase activity, did not
169 change the number of lamellipodia compared infected cells treated with vehicle **(Fig. 3A)**. These
170 results indicate that IRE1 can control migration of *Toxoplasma* infected cells independent of its
171 known enzymatic activities.

172 The functions of filamin A in cytoskeleton dynamics and cell migration is dependent on
173 phosphorylation of serine 2,152 (S2152) [21]. We detected a sharp increase in filamin A
174 phosphorylation in MEF cells infected with *Toxoplasma* for 18 h, which was not observed in
175 host cells lacking IRE1 **(Fig. 3B)**. To address whether there is an association between IRE1 and
176 filamin A, we expressed myc-tagged filamin A (myc-FLNA) in WT MEF cells. Following 18 h
177 of *Toxoplasma* infection, we then performed an immunoprecipitation (IP) of the tagged filamin
178 A, followed by immunoblot measurements of associated IRE1. There was enhanced association
179 of IRE1 with filamin A in cells infected with the parasite compared to those uninfected **(Fig.**
180 **3C)**.

181 Next, we measured changes in host cell transmigration upon parasite infection and
182 determined that there was a 2-fold increase in migration of WT MEF cells upon infection with
183 *Toxoplasma* **(Fig. 3D, Fig. S3B)**. Increased host cell migration was observed regardless of
184 whether the cells were infected with type I RH or type II ME49 strain parasites **(Fig. S3C)**. In
185 contrast, parasite infection did not induce migration of cells lacking IRE1. Levels of migration in
186 infected WT MEF cells treated with the IRE1 enzymatic inhibitors, KIRA6 or 4μ8c, or an ATF6
187 inhibitor (Ceapin-A7), were not significantly changed compared to untreated infected MEF cells,
188 nor were they altered in cells lacking the downstream IRE1 target XBP1 **(Fig. 3D).** Notably,

Toxoplasma-induced migration of PERK-deficient cells or WT treated with PERK inhibitor was increased >2.5-fold upon parasite infection compared to infected cells with functional PERK **(Fig. 3D)**. These results suggest that IRE1 plays a critical role in inducing migration of *Toxoplasma*-infected cells and that this migration is independent of the protein kinase and endoribonuclease activities of IRE1 and its downstream target *XBP1*. Furthermore, PERK is suggested to dampen both IRE1 functions in *XBP1* mRNA splicing and cell migration, which are induced upon *Toxoplasma* infection.

ER stress induces cell migration by mechanisms involving IRE1 oligomerization

To better understand the mechanisms by which IRE1 enhances host cell migration in response to *Toxoplasma* infection, we rescued the *IRE1*$^{-/-}$ cells by expressing WT or defined mutant versions of IRE1 **(Fig. 3E)**. Equal amounts of the IRE1 proteins were expressed as judged by immunoblot and immunofluorescence analyses **(Fig. S4A and B)**. As expected, *ire1-wt* rescued the migration capacity of infected cells **(Fig. 3E).** Expression of IRE1 defective in kinase (*ire1-kD*) or endoribonuclease (*ire1-eD*) activities still rescued the migration phenotype, further supporting the idea that these activities are dispensable for induced cell migration in response to parasite infection **(Fig. 3E)**. In contrast, cells expressing IRE1 with mutations in the oligomerization domain (*ire1-oD*) were deficient in *Toxoplasma*-induced migration **(Fig. 3E)**. Furthermore, a truncated c-terminal version of IRE1 (*ire1-Δ965)* lacking the proline-rich carboxy-terminal segment of IRE1 that binds filamin A [12] was also impaired in cell migration following infection **(Fig. 3E)**. As anticipated, only *ire1-wt* and *ire1-Δ965* showed induction of spliced *XBP1* mRNA upon pharmacological induction of ER stress **(Fig. S4C)**. These results suggest that *Toxoplasma* infection induces IRE1 oligomerization (see also Fig. 1B), and that the

212 hypermigratory behavior of infected host cells is reliant on both the oligomerization domain and
213 the portion of IRE1 that interacts with filamin A.

214 Since we found that *Toxoplasma* induces calcium release from the host ER upon
215 infection, we examined the importance of calcium release in host cell migration induced by
216 *Toxoplasma*. We treated infected cells with RyR and IP_3R receptor blockers or activators during
217 the migration assay: ryanodine (Ry) or xestospongin-C (XeC) were used to inhibit RyR and IP_3R
218 receptors, respectively; caffeine or IP_3 were used to activate RyR and IP_3R receptors,
219 respectively. When infected cells were treated with the RyR and IP_3R activators (releasing
220 calcium from ER into the cytosol), the migration levels increased compared to cells not treated
221 with these agents. By contrast, addition of the IP_3R inhibitor significantly decreased migration of
222 the infected cells **(Fig. 3F)**, consistent with IP_3R being the major calcium release receptor
223 involved in triggering the host UPR following *Toxoplasma* infection **(Fig. 2B)**. These results
224 support the idea that calcium release from the host ER contributes to IRE1 activation and its
225 subsequent role in augmenting migration in response to infection.
226
227 **IRE1 controls host cell migration in infected immune cells *in vitro*.**
228 *Toxoplasma* makes use of immune cells as a "Trojan Horse" to disseminate to distal
229 organs and tissues throughout the body of the infected host [13]. To address whether *Toxoplasma*
230 is targeting IRE1 in immune cells to enhance their migration and facilitate dissemination, we
231 infected bone marrow-derived dendritic cells (DCs) with *Toxoplasma*. Levels of *XBP1s* mRNA
232 were sharply increased upon *Toxoplasma* infection in DCs **(Fig. 4A)**, consistent with the idea
233 that the parasite infection activated IRE1 in this cell type. Next, we used CRISPR/Cas9 and two
234 distinct sgRNAs (sgRNA 1 and 2) to disrupt IRE1 in DCs **(Fig. S5A)**. The sgRNA1 and sgRNA2

decreased *IRE1* mRNA levels by 66% and 93%, respectively **(Fig. 4B)**. Each gRNA also led to a corresponding reduction in IRE1 protein in DCs, with sgRNA2 leading to no detectable IRE1 **(Fig. 4C)**. IRE1-depleted DCs (ire1 (-)) did not exhibit decreased cell viability compared to WT, nor did they show any difference in infectivity with *Toxoplasma* **(Fig. 4D, Fig. S5B)**. However, loss of IRE1 in DCs significantly lowered the transmigratory capacity following infection with either Type I or Type II strains of *Toxoplasma* **(Fig. 4E, Fig. S3D)**. To determine whether IP_3R plays a role in the migration of infected DCs, we carried out the migration assay in the presence of XeC. Inhibition of IP_3R resulted in a loss of host cell migration following 18 h of *Toxoplasma* infection **(Fig. 4F)**, further supporting the importance of calcium homeostasis in the ER for migration of *Toxoplasma* infected cells. To test whether IRE1 controls the migration of infected macrophages as well, we used CRISPR/Cas9 to deplete IRE1 in J774.1 macrophages **(Fig. 4G and H)**. As observed for DCs, the loss of IRE1 significantly reduced the ability of infected macrophages to migrate **(Fig. 4I)**.

IRE1 facilitates dissemination of *Toxoplasma in vivo*

To determine the importance of IRE1 in the migration of infected DCs *in vivo*, we inoculated C57BL/6 mice intraperitoneally (i.p.) with infected WT or infected ire1 (-) DCs and measured parasite burden in the spleen by PCR at the designated time intervals over 3 days. Depletion of IRE1 in the DCs by CRISPR/Cas9 was confirmed by RT-qPCR and immunoblot analyses **(Fig. 5A and B).** Moreover, we ascertained that there was no significant difference in parasite infection of WT and IRE1-depleted DCs **(Fig. 5C)**. *Toxoplasma* was first detected in the spleens of mice 12 h following i.p. inoculation with infected WT DCs, increasing at each time point over the 3-day period **(Fig. 5D)**. In striking contrast, appreciable levels of *Toxoplasma*

dissemination of infected IRE1-depleted DCs to the spleen were not detected until 3 days following inoculation of the mice **(Fig. 5D)**. Even at the 3-day time point, the loss of IRE1 from DCs produced lowered levels of parasitemia in the spleen that were similar to those measured at 12 h of infected WT DCs. We also measured the *Toxoplasma* dissemination to the brain at 3 days, finding 200-fold fewer parasites when infected IRE1-depleted DCs were inoculated into the mice **(Fig. 5E)**. Mice inoculated with infected DCs lacking IRE1 survived significantly longer than mice receiving infected WT DCs **(Fig. 5F)**. These results demonstrate a novel role for host IRE1 in parasite pathogenesis, as IRE1 is crucial for the migration of immune cells being co-opted as "Trojan Horses" for parasite dissemination.

Discussion

Obligate intracellular pathogens create a niche inside of their host cell that allows for parasite protection, nutrient acquisition, and the controlled release of pathogen effectors that promote infection and dissemination. *Toxoplasma* tachyzoites reside inside of a nonfusogenic parasitophorous vacuole (PV) that forms intimate contacts with host organelles and vesicles, including the ER and mitochondria [4, 5]. It is suggested that the recruitment of host organelles to the PV allows *Toxoplasma* to control critical host cell operations, including antigen presentation, nutrient production, and suppression of apoptosis [5]. In this study, we addressed consequences of the *Toxoplasma*-ER engagement on parasite infection and dissemination in the host. As illustrated in a model presented in **Fig. 5G**, we showed that *Toxoplasma* infection activates each of the UPR sensor proteins, including IRE1, via ER stress that results at least in part from release of calcium from the organelle, primarily through IP_3R. In addition to its role in the UPR, IRE1 has recently been shown to have noncanonical functions associated with the

remodeling of the cytoskeleton through direct interactions with the actin crosslinking factor filamin A [12]. We showed that *Toxoplasma* alters the morphology of its host cells through IRE1-filamin A interactions, which directs cytoskeletal remodeling that contributes to a hypermigratory phenotype that facilitated dissemination of the parasite into multiple organs of the infection host. The role of IRE1 in *Toxoplasma*-induced hypermigration is not reliant on its protein kinase or endoribonuclease activities that are central for classical UPR signaling; rather, it is IRE1 oligomerization and the C-terminal residues required for filamin A association that prove to be important.

After oral infection, *Toxoplasma* rapidly spreads from the lamina propria to distal organs using host immune cells as a vehicle for dissemination [22]. Given our discovery that IRE1 is mobilized by *Toxoplasma* to enhance hypermigratory behavior in host cells, we tested whether IRE1 is crucial to *in vivo* dissemination in a mouse model of infection. We found that depletion of IRE1 in immune cells sharply decreases the number of parasites in the spleen or brain of infected mice **(Fig. 5E)**. These results reveal a number of potential new targets for drug development aimed at thwarted spread of infection in the body.

It is noteworthy that other mechanisms have been suggested to contribute to the cell hypermotility upon *Toxoplasma* infection. For example, parasite effector protein TgWIP, TIMP-1, and GABAergic signaling were reported to signal hypermigration of certain infected host cells [23-26]. A key question for future studies is how these different mechanisms are coordinated to induce hypermigratory activity in *Toxoplasma*-infected host cells.

Methods

Host cell and parasite culture. MEF (mouse embryonic fibroblast) cells were cultured in Dulbecco's modification of Eagle's medium (DMEM) supplemented with 10% heat-inactivated fetal bovine serum (FBS) (Gibco/Invitrogen) and penicillin/streptomycin at 37°C with 5% CO_2. *PERK*$^{-/-}$ cells were previously reported [27] and IRE1-deficient MEF cells were engineered by CRISPR as described below. Host cells were seeded at a density of $2x10^5$ cells/well in a 6 well plate and cultured for 18 h. Infection was performed using multiplicity of infection (MOI) of 3 with Type I or II (RH or ME49) strain *Toxoplasma* parasites, as indicated, for 18 h. The infected cells were cultured in DMEM medium supplemented with 10% heat-inactivated fetal bovine serum (FBS) (Gibco/Invitrogen) and penicillin/streptomycin at 37°C with 5% CO_2. Cultures of DCs and J774.1 macrophages were cultivated in Roswell Park Memorial Institute (RPMI) supplemented with 10% heat-inactivated fetal bovine serum (FBS) (Gibco/Invitrogen) and penicillin/streptomycin at 37°C with 5% CO_2 and infected as described above.

Generation of *IRE1* knockout cells. Disruption of the *IRE1* gene in MEF cells was carried out using the CRISPR/Cas9 method [28]. Two distinct sgRNAs designed using DESKGEN™ toll (g1-TGGACACGGAGCTGACT and g2-ACACGGAGCTGACTGGG) were examined individually. The sgRNAs were prepared using the EnGen™ sgRNA Synthesis Kit (New England BioLabs), along with a sg control (g-control- CATCCTCGGCACCGTCACCC). The sgRNAs were then associated with EnGen® Spy Cas9 NLS protein (New England BioLabs) at room temperature for 20 min. MEF cells were then transfected with the bound sgRNA/Cas9 protein using the Lipofectamine CRISPRMAX Cas9 Transfection Reagent (Thermo-Fisher Scientific). After culturing the transfected cells for 48 h, 100 cells were plated in 10 mm tissue-

culture dishes for cloning. Cloned *IRE1*$^{-/-}$ MEF cells were validated by RT-qPCR using specific primers and by immunoblot using IRE1-specific antibody (Abcam-ab37073). *IRE1*$^{-/-}$ cells were complemented with pcDNA3-derived vectors containing WT or the indicated mutant versions of *IRE1*. Briefly, the mouse cDNA sequence of *IRE1* from MEF cells was inserted into pcDNA3-EGFP plasmid (Addgene #13031), resulting in fusion proteins with the EGFP fused to the carboxy terminus of IRE1. Mutations in *IRE1* include changes inactivating the critical functions, including *kD* (kinase domain- K599A), *eD* (endoribonuclease domain- P830L), *oD* (oligomerization domain- D123P) or *c-terminal* (truncated c-terminal Δ965), were carried out using specific primers **(Supplemental Table 1)** and the Q5 Site-Directed Mutagenesis Kit (New England Biolabs). After sequence verification, the plasmids were transfected into *IRE1*$^{-/-}$ cells using FuGENE 6 Transfection Reagent. Rescued WT and mutant IRE1 protein expression were confirmed by immunoblot and immunofluorescence microscopy **(Fig. S4A and B)**.

To generate bone marrow-derived dendritic cells (DCs), 10 x 10^6 bone marrow cells were isolated and cultured in 6-well plate in 3 ml of complete medium (RPMI 1640 medium supplemented with 10% fetal bovine serum, penicillin, streptomycin, glutamine, 2-mercaptoethanol, 20 ng/ml granulocytes-macrophage colony-stimulating factor (GM-CSF) and 5ng/ml Interleukin 4 (IL-4) (both from Peprotech)) for 7 days. Half of the medium was replaced every two days with medium supplemented with GM-CSF and IL-4, as previously described [29]. DCs or J774.1 macrophages were transfected with IRE1-sgRNA-1 or 2, associated with EnGen™ Spy Cas9 NLS protein (New England BioLabs), using the 4D-Nucleofector™ System (Lonza) in combination with the P3 Primary Cell 4D-Nucleofector™ X Kit. After 48 h, the *IRE1* mRNA and protein levels were measured by RT-qPCR and immunoblot, respectively. Viability of DCs was examined by trypan blue staining.

Measurement of mRNA levels. Cells were first infected with *Toxoplasma* for 2 h, washed with phosphate-buffered saline (PBS), and then cultured in DMEM at the indicated time points. RNA was isolated from cells using TRIzol LS Reagent (Invitrogen™), the cDNA was then generated using Omniscript (Qiagen) and RT-qPCR was performed using SYBR® Green Real-Time PCR Master Mixes (Invitrogen™) and the StepOnePlus Real System (Applied Biosystems™). Oligonucleotide primers used to measure each target mRNA is listed in the supplementary Table 1. Relative levels of target mRNAs from the uninfected samples were adjusted to 1 and served as the basal control value. Values of each time point were normalized to mock infection. Each experiment was performed three times, each with three technical replicates.

Immunoblot analyses. Cells were infected with *Toxoplasma* for 2 h, washed with PBS, then cultured in DMEM for the indicated time points. The infected cells were harvested in RIPA buffer solution supplemented with cOmplete™ and EDTA-free Protease Inhibitor Cocktail (Roche). Protein quantification was performed using the Bradford Reagent (Sigma-Aldrich). Equal amounts of protein lysates were separated by SDS-PAGE and proteins were transferred to nitrocellulose filters. Immunoblot analyses were using primary antibodies- IRE1 (Abcam-ab37073), XBP1s (Cell Signaling #D2C1F), ATF6 [30], GAPDH (Abcam-ab9485), PERK (Cell Signaling #3192), followed by Amersham ECL HRP-Conjugated Antibodies secondary antibody. These antibodies and additional reagents used in the study are listed in the supplementary Table 2. Proteins were visualized in the immunoblots were visualized using FluorChem M- Multiplex fluorescence (Protein Simple). Immunoblot analyses were carried out for three independent experiments.

Calcium measurement assay. *Toxoplasma*-infected MEF cells were washed twice with buffer A solution supplemented with glucose (120 mM NaCl, 20 mM HEPES (pH 7.4), 4.7 mM KCl, 1.2 mM NaH_2PO_4, 1.2 mM $MgSO_4$, 1.2 mM $CaCl_2$ and 10 mM glucose) [31], and then a final concentration of 5 µM of Fluo-4, AM (Thermo Fisher Scientific, F14201) was added for 15 min at 37°C. Prior to the calcium measurements, cells were washed once with buffer A solution supplemented with glucose. A Synergy (BioTek) plate reader was used to monitor the Fluo-4 AM fluorescence at 488-nm excitation and 524-nm emission wavelengths. Values derived from infected cells (ΔF) were divided by the resting intracellular calcium (Fo), ΔF/Fo, and the values of each time point were normalized to mock-infected cells. In parallel, live infected cells were imaged by microscopy at the same exposure and a heat map was generated using ImageJ software. To determine the activity of RyR and IP_3R receptors, infected cells were incubated with 5 µM Mag-Fluo-4, a low-affinity Ca^{2+} indicator, then permeabilized with 10 µg/ml of saponin followed by incubation with 1.5 mM ATP to maintain Mag-Fluo-4 in the ER [19] **(Fig. S2B)**. Infected cells were treated with the indicated concentrations of caffeine (RyR, 0-200 mM) or IP_3 (IP_3R, 0-3 µM) (Sigma-Aldrich). A Synergy (BioTek) plate reader was used to monitor the Mag-Fluo-4 fluorescence at 490-nm excitation and 525-nm emission wavelengths [19]. Values were normalized to mock-infected cells.

Immunofluorescence assay. Cultured cells were infected with *Toxoplasma* for 18 h, then fixed with 2.5% paraformaldehyde for 20 min and blocked with PBS supplemented with 2% BSA. Cells were permeabilized in blocking solution containing 0.01% Triton X-100 for 30 min, and incubated with primary antibody (SAG1-p30, Invitrogen) for 1 h. Secondary goat anti-rabbit

Alexa-fluor 488 (Invitrogen) was applied for 1 h in the presence of Rhodamine Phalloidin (Thermo Fisher Scientific) followed by Prolong Gold antifade reagent (Invitrogen). DAPI was used to visualize host cells and parasite nuclei (Vector Labs). Images were acquired with a Leica inverted DMI6000B microscope with 63x oil immersion objective and analyzed in ImageJ. Alternatively, *IRE1*$^{-/-}$ cells were transfected with pcDNA3 encoding IRE1 fused with EGFP at the carboxy terminus and infected with *Toxoplasma* for 18h (MOI: 3); the cells were then fixed and imaged as described above.

Immunoprecipitation assay. The mouse cDNA sequence of filamin A from MEF cells was amplified and cloned into pcDNA3-myc plasmid (Addgene). The resulting plasmid pcDNA3-myc-FLNA was transiently transfected in the MEF cells and then the transfected cells were infected with *Toxoplasma* for 18 h (MOI: 3). Cell lysates were prepared using IP-lysis solution (0.5% NP-40, 250 mM NaCl, 30 mM Tris, 0.5% glycerol, pH 7.4, 250 mM phenylmethylsulfonyl fluoride (PMSF) supplemented with cOmplete™ and EDTA-free Protease Inhibitor Cocktail (Roche)). To immunoprecipitate myc-tagged filamin A (myc-filamin A), equal amounts of protein lysates were incubated with IgG Magnetic beads (Pierce) for 2 h, then mixed with anti-myc Magnetic beads (Pierce) overnight at 4 °C with rotation. Proteins bound to the beads were subsequently washed four times with IP-lysis solution at 4°C and then once with IP-lysis solution supplemented with 500 mM NaCl. Protein complexes were eluted at 95°C for 5 min in loading buffer solution and then separated by SDS-PAGE, followed by immunoblot analyses using specific antibodies to IRE1 (Abcam-ab37073) or Myc (Cell Signaling #2276).

418 **Cell migration assay.** Cells were infected with *Toxoplasma* MOI 3 for 18 h and then trypsinized
419 and counted using a hemocytometer; $2x10^4$ cells were resuspended in serum-free medium and
420 applied to the top of a membrane coated with collagen I (rat-tail) (Gibco- A1048301).
421 Transmigration assays were carried out using a Corning Transwell Costar apparatus (6.5 mm
422 diameter and 8 μm pore size) as described [32]. After 18 h for MEF and 6 h for DCs and
423 macrophages, the medium was removed, and the cells were fixed with 2.5% paraformaldehyde
424 for 20 min. The facilitate counting of migrated cells, cells that did not migrate and remained on
425 the upper side of membrane (unmigrated cells) were removed with a swab. The membrane was
426 incubated with Prolong Gold antifade reagent with DAPI. Cells were counted using a Leica
427 inverted DMI6000B microscope with 63x oil immersion objective. The transmigration was
428 determined by numbers of migrated infected cells in 5 fields normalized to number of uninfected
429 cells. Each transmigration assay was carried out in technical triplicate in n=3.
430
431 ***In vivo* migration assay.** DCs were plated in 6-well plates ($1x10^6$ cells/well) and allowed to
432 adhere overnight. DCs were infected with *Toxoplasma* for 1 h (MOI: 3) and then washed with
433 RPMI to remove extracellular parasites. After 18 h, infected DCs were incubated with
434 CellTracker™ Orange CMTMR (Thermo Fisher) as described [33]. Infected DCs were
435 intraperitoneally inoculated into 6-weeks-old female C57BL/6J mice whose spleens and brains
436 were subsequently harvested at the indicated time points and the DC migration to the spleen was
437 measured by the fluorescence intensity at the indicated time points using a Synergy (BioTek)
438 plate reader at ex/em 541/565 nm **(Fig. S5C)**. Also, DNA was isolated from the spleen and brain
439 using TRIzol (Thermo Fisher), and the number of parasites was determined by using a PCR-
440 based method measuring levels of the parasite-specific gene region B1 as previously described

441 [34]. After 3 days, the mice were observed twice a day and percent survival was recorded at each
442 time point. The mice experiment, including parasite measurement by B1 were performed on
443 blinded. The mice used in this study were housed in American Association for Accreditation of
444 Laboratory Animal Care (AAALAC)-approved facilities at the Indiana University School of
445 Medicine Laboratory Animal Research Center (LARC). The Institutional Animal Care and Use
446 Committee (IACUC) at Indiana University School of Medicine approved the use of all animals
447 and procedures (IACUC protocol number 11376).
448
449 **Quantification and statistical analysis.** Quantitative data were presented as the mean and
450 standard deviation and were derived from three biological replicates. Statistical significance was
451 determined using One-way ANOVA with Tukey's post hoc test and multiple t-test two-tailed
452 using Graph Prism software. The number of biological replicates (n) and p-values are indicated
453 in figure legends. For immunoblot analyses, the reported images are representative of at least
454 three independent experiments. The mice survival curve was analyzed by Gehan-Breslow-
455 Wilcoxon test for *in vivo* analysis.

Acknowledgments

This research was supported by a research grant from National Institutes of Health (AI124723 to W.J.S. and R.C.W.). R.C.W. receives financial support from HiberCell. M.H.K. and N.S.A. were supported by funds from the Brown Center for Immunotherapy. J.M. was supported by PHS grant T32 AI060519 and the Joseph and Lucille Madri Family Scholarship. The authors would like to thank Drs. Tatiana Clemente and Stacey Gilk, as well as our lab members for helpful discussions.

Contributions

Study design and planning: L.A., J.M., P.H.A., M.H.K, R.C.W. and W.J.S. Performed experiments and generated reagents: L.A., J.M., P.H.A. and N.S.A. Data analysis: L.A., J.M. and P.H.A. Manuscript writing: L.A., R.C.W. and W.J.S. Manuscript was drafted with input from all authors.

Competing interests

The authors declare no competing interests.

References

1. Hakimi, M.A. et al. (2017) Toxoplasma Effectors Targeting Host Signaling and Transcription. Clin Microbiol Rev 30 (3), 615-645.

2. Jeffers, V. et al. (2018) A latent ability to persist: differentiation in Toxoplasma gondii. Cell Mol Life Sci 75 (13), 2355-2373.

3. Blader, I.J. and Koshy, A.A. (2014) Toxoplasma gondii development of its replicative niche: in its host cell and beyond. Eukaryot Cell 13 (8), 965-76.

4. Sinai, A.P. et al. (1997) Association of host cell endoplasmic reticulum and mitochondria with the Toxoplasma gondii parasitophorous vacuole membrane: a high affinity interaction. J Cell Sci 110 (Pt 17), 2117-28.

5. Coppens, I. and Romano, J.D. (2018) Hostile intruder: Toxoplasma holds host organelles captive. PLoS Pathog 14 (3), e1006893.

6. Walter, P. and Ron, D. (2011) The unfolded protein response: from stress pathway to homeostatic regulation. Science 334 (6059), 1081-6.

7. Karagoz, G.E. et al. (2019) The Unfolded Protein Response: Detecting and Responding to Fluctuations in the Protein-Folding Capacity of the Endoplasmic Reticulum. Cold Spring Harb Perspect Biol 11 (9).

8. Hetz, C. and Papa, F.R. (2018) The Unfolded Protein Response and Cell Fate Control. Mol Cell 69 (2), 169-181.

9. Mori, K. (2010) Divest yourself of a preconceived idea: transcription factor ATF6 is not a soluble protein! Mol Biol Cell 21 (9), 1435-8.

10. Wek, R.C. (2018) Role of eIF2alpha Kinases in Translational Control and Adaptation to Cellular Stress. Cold Spring Harb Perspect Biol 10 (7).

11. Chang, T.K. et al. (2018) Coordination between Two Branches of the Unfolded Protein Response Determines Apoptotic Cell Fate. Mol Cell 71 (4), 629-636 e5.

12. Urra, H. et al. (2018) IRE1alpha governs cytoskeleton remodelling and cell migration through a direct interaction with filamin A. Nat Cell Biol 20 (8), 942-953.

13. Bierly, A.L. et al. (2008) Dendritic cells expressing plasmacytoid marker PDCA-1 are Trojan horses during Toxoplasma gondii infection. J Immunol 181 (12), 8485-91.

14. Korennykh, A.V. et al. (2009) The unfolded protein response signals through high-order assembly of Ire1. Nature 457 (7230), 687-93.

15. Aragon, T. et al. (2009) Messenger RNA targeting to endoplasmic reticulum stress signalling sites. Nature 457 (7230), 736-40.

16. Li, H. et al. (2010) Mammalian endoplasmic reticulum stress sensor IRE1 signals by dynamic clustering. Proc Natl Acad Sci U S A 107 (37), 16113-8.

17. Carreras-Sureda, A. et al. (2018) Calcium signaling at the endoplasmic reticulum: fine-tuning stress responses. Cell Calcium 70, 24-31.

18. Carreras-Sureda, A. et al. (2019) Non-canonical function of IRE1alpha determines mitochondria-associated endoplasmic reticulum composition to control calcium transfer and bioenergetics. Nat Cell Biol 21 (6), 755-767.

19. Yamamoto, W.R. et al. (2019) Endoplasmic reticulum stress alters ryanodine receptor function in the murine pancreatic beta cell. J Biol Chem 294 (1), 168-181.

20. Weidner, J.M. et al. (2013) Rapid cytoskeleton remodelling in dendritic cells following invasion by Toxoplasma gondii coincides with the onset of a hypermigratory phenotype. Cell Microbiol 15 (10), 1735-52.

517 21. Zhou, A.X. et al. (2010) Filamins in cell signaling, transcription and organ development.
518 Trends Cell Biol 20 (2), 113-23.
519 22. Drewry, L.L. and Sibley, L.D. (2019) The hitchhiker's guide to parasite dissemination.
520 Cell Microbiol, e13070.
521 23. Olafsson, E.B. et al. (2019) TIMP-1 promotes hypermigration of Toxoplasma-infected
522 primary dendritic cells via CD63-ITGB1-FAK signaling. J Cell Sci 132 (3).
523 24. Bhandage, A.K. et al. (2019) Toxoplasma-Induced Hypermigration of Primary Cortical
524 Microglia Implicates GABAergic Signaling. Front Cell Infect Microbiol 9, 73.
525 25. Bhandage, A.K. and Barragan, A. (2019) Calling in the CaValry-Toxoplasma gondii
526 Hijacks GABAergic Signaling and Voltage-Dependent Calcium Channel Signaling for Trojan
527 horse-Mediated Dissemination. Front Cell Infect Microbiol 9, 61.
528 26. Sangare, L.O. et al. (2019) In Vivo CRISPR Screen Identifies TgWIP as a Toxoplasma
529 Modulator of Dendritic Cell Migration. Cell Host Microbe 26 (4), 478-492.e8.
530 27. Jiang, H.Y. et al. (2004) Activating transcription factor 3 is integral to the eukaryotic
531 initiation factor 2 kinase stress response. Mol Cell Biol 24 (3), 1365-77.
532 28. Cong, L. et al. (2013) Multiplex genome engineering using CRISPR/Cas systems.
533 Science 339 (6121), 819-23.
534 29. Inaba, K. et al. (2001) Isolation of dendritic cells. Curr Protoc Immunol Chapter 3, Unit
535 3.7.
536 30. Teske, B.F. et al. (2011) The eIF2 kinase PERK and the integrated stress response
537 facilitate activation of ATF6 during endoplasmic reticulum stress. Mol Biol Cell 22 (22), 4390-
538 405.

539 31. Borges-Pereira, L. et al. (2015) Calcium Signaling throughout the Toxoplasma gondii
540 Lytic Cycle: A STUDY USING GENETICALLY ENCODED CALCIUM INDICATORS. J
541 Biol Chem 290 (45), 26914-26.
542 32. Lechuga, S. et al. (2019) Adducins inhibit lung cancer cell migration through
543 mechanisms involving regulation of cell-matrix adhesion and cadherin-11 expression. Biochim
544 Biophys Acta Mol Cell Res 1866 (3), 395-408.
545 33. Lambert, H. et al. (2006) Induction of dendritic cell migration upon Toxoplasma gondii
546 infection potentiates parasite dissemination. Cell Microbiol 8 (10), 1611-23.
547 34. Kompalic-Cristo, A. et al. (2007) Evaluation of a real-time PCR assay based on the
548 repetitive B1 gene for the detection of Toxoplasma gondii in human peripheral blood. Parasitol
549 Res 101 (3), 619-25.
550
551

Figure Legends

Figure. 1. *Toxoplasma* infection triggers activation of the UPR in host cells. (A) At the indicated times following infection with *Toxoplasma*, cells were harvested and the levels of total PERK, PERK-P, full length ATF6 and ATF6-N, XBP1s, and GAPDH were measured by immunoblot analyses. (B) *IRE1*$^{-/-}$ MEF cells were transfected with a plasmid encoding EGFP-IRE1 (green), followed by infection with *Toxoplasma*. DAPI (blue) was used to visualize host cell and parasites nuclei. Two boxed areas (1 and 2) of each condition are amplified to highlight the IRE1 distribution. Bar=5 µm. (C) MEF cells were infected with *Toxoplasma* for 18 h, or were mock infected, and the mRNA levels of the indicated ERAD/chaperone genes were measured by RT-qPCR. Levels of mRNA were normalized to mock infected, which is represented as a value of 1. (±SD, n=3) ***p<0.001, ****p< 0.0001. (D) *XBP1s* mRNA levels were measured by RT-qPCR at the indicated hpi in WT, *PERK*$^{-/-}$ and *IRE1*$^{-/-}$ MEF cells, as indicated. Levels of *XBP1s* mRNA were normalized to total *XBP1* mRNA in mock infected cells (value of 1) at each time point. (±SD, n=3) ****p<0.0001.

Figure. 2. *Toxoplasma* infection induces calcium release. (A) At the indicated time hpi, cytosolic calcium levels were measured in the infected WT and *IRE1*$^{-/-}$ cells. Values of infected cells were normalized to mock-infected cells (±SD, n=3), **p<0.005 and ****p<0.001. (B) Infected WT and *IRE1*$^{-/-}$ cells were treated with RyR or IP_3R inhibitors for 6 h and the levels of cytosolic calcium were measured. 100 µM Ryanodine (RyR inhibitor) and 0.6 µM Xestospongin C (XeC) (IP_3R inhibitor), (±SD, n=3) **p<0.05, ***p<0.005. Infected cells were incubated with Mag-Fluo-4, followed by plasma membrane permeabilization with saponin and incubation with ATP to maintain the calcium in the ER. To estimate RyR (C) and IP_3R (D) activity, WT and

575 *IRE1*$^{-/-}$ cells infected with *Toxoplasma* for 18 h were treated with caffeine or IP_3 at the indicated
576 concentrations and calcium release is represented the fluorescence using Mag-Fluo-4 as
577 described [19]. Values are represented as the percentage of calcium release and the respective
578 start points were normalized to untreated WT and *IRE1*$^{-/-}$ cells, respectively. (±SD, n=3),
579 **p<0.05, ****p<0.001.
580
581 **Figure. 3. Activation of IRE1 enhances migration of cells infected with *Toxoplasma*.** (A) The
582 numbers of lamellipodia were determined in 50 randomly selected MEF cells infected with
583 *Toxoplasma* 18 hpi and normalized to uninfected cells. Also shown are infected WT cells treated
584 with 1.2 µM PERKi (GSK2656157), 0. 4 µM 4µ8c, 250 nM KIRA6, or 0.2 µM ceapin-A7 for 18
585 h. (±SD, n=5) **p<0.05, ***p<0.005. (B) WT and *IRE1*$^{-/-}$ cells were infected with *Toxoplasma*
586 for 18 h, then cells were harvested and the levels of filamin A phosphorylation (S2152) were
587 measured by immunoblot analyses. (C) WT cells transiently expressing Myc-filamin A were
588 infected with *Toxoplasma* for 18 h. IP of the tagged Filamin A was carried out using Myc
589 magnetic beads. Bound proteins were separated by SDS-PAGE and the levels of Myc-filamin A
590 and associated IRE1 were measured by immunoblot and compared to uninfected cells.
591 Densitometry of IRE1 signal divided by Myc signal (IRE1/Myc). (D) WT or *IRE1*$^{-/-}$, *PERK*$^{-/-}$,
592 and *XBP1*$^{-/-}$ cells were infected with *Toxoplasma* for 18 h. Alternatively, WT cells were infected
593 with parasite and treated with the following inhibitors during migration per 18 h: 1.2 µM PERKi
594 (GSK2656157), 0.2 µM Ceapin-A7, 250 nM KIRA6, or 0.4 µM 4µ8c. Infected and mock
595 infected cells were trypsinized, counted, and the same number of cells was used for the
596 transmigration assay. Transmigration was determined by counting the number of infected
597 normalized to noninfected cells that migrated through the membrane. (±SD n=3), *** p<0.0005.

598 (E) *IRE1*$^{-/-}$ cells were rescued with *ire1-wt* (wild-type), *kD* (kinase domain-dead- K599A), *eD*
599 (endoribonuclease domain-dead- P830L), *oD* (oligomerization domain-dead- D123P) or *Δ965*
600 (truncated c-terminal *Δ965*), and then a transmigration assay was carried out as described above.
601 (±SD, n=3), ****p<0.0001. (F) Transmigration assay of infected WT MEF cells was carried out
602 in the presence of IP_3R and RyR inhibitors (0.6 μM Xestospongin C, XeC or 100 μM
603 Ryanodine, Ry) or activators (100 μM IP_3 or 1 mM caffeine). (±SD, n=3), *p<0.1, **p<0.05 and
604 ***p<0.0005. ns = not significant.
605
606 **Figure. 4. IRE1 is important for migration of infected DCs.** (A) Bone marrow-derived DCs
607 were infected with *Toxoplasma* for 18 h and *XBP1s* mRNA levels were measured by RT-qPCR.
608 The values of XBP1s were normalized to values of total XBP1. (±SD, n=3) ***p<0.0005. (B-C)
609 The CRISPR/Cas9-engineered depletion of IRE1 in DCs, designated ire (-), was assayed by RT-
610 qPCR and immunoblot using IRE1 antibody compared to WT cells (GAPDH was included as a
611 loading control). (D) Percentage of infection was determined by counting the number of parasites
612 inside 100 WT or ire1 (-) cells. (E) WT and ire1 (-) cells were infected for 18 h and the
613 transmigration assay was carried out for 6 h. Transmigration was determined by counting the
614 number of infected cells normalized to noninfected cells. (±SD, n=3), **p<0.05 and
615 ***p<0.0005. (F) WT-DCs were infected for 18 h and the transmigration assay was carried out
616 in presence of 0.6 μM xestospongin C (XeC) for 6 h (±SD, n=3), ***p<0.001. (G-H) J774.1
617 macrophages were transfected with sgRNA-2 and the depletion of IRE1 was assayed by RT-
618 qPCR and immunoblot as described in (C). (I) At 18 hpi, WT or ire1 (-) J774.1 macrophages
619 were assayed for transmigration as described above. (±SD, n=3), **p<0.05.
620

Figure. 5. IRE1 facilitates migration of infected DCs *in vivo*. (A-B) IRE1 was depleted in bone marrow-derived DCs by CRISPR/Cas9 and loss of *IRE1* expression was assayed by RT-qPCR and immunoblot analyses. (C) WT or ire1 (-) DCs were infected for 18 h and the percentage of infection was determined by counting the number of parasites in 100 cells. (D) Infected WT and ire1 (-) cells were inoculated into mice by i.p. injection (10^6 infected cells). At the indicated hpi, the spleen of each mouse was harvested, and the number of parasites was determined by PCR. ***p<0.005 and ****p<0.0001. (E) At 3 days post inoculation, the number of parasites was determined in the brain using PCR. ****p<0.0001. (F) Survival of C57BL/6 mice challenged with 10^6 infected WT or ire 1 (-) DCs. ***p<0.0005. Statistical analyses by Gehan-Breslow-Wilcoxon test. (G) Model for IRE1-direct hypermigration of host cells infected by *Toxoplasma*. During infection, *Toxoplasma* triggers calcium release from the host ER, which creates ER stress and induction of the UPR, which results in enhanced IRE1 association with filamin A. Consequently, the IRE1-filamin A interaction promotes actin remodeling and host cell migration.

Supplemental Figure Legends

Supplemental Figure. 1. MEF cells were transfected with Cas9 bound to sgRNA targeted to IRE1 as described in the methods section; lowered *IRE1* expression resulting from the CRISPR/Cas9 gene editing was evaluated by (A) RT-qPCR and (B) immunoblot analyses. GAPDH was included as a loading control for the immunoblot analyses. (C) WT and *IRE1*$^{-/-}$ MEF cells were treated with 1 µM thapsigargin (TG), or no stress agent, for 6 h. Cells were then harvested and the *XBP1s* mRNA levels were measured by RT-qPCR. The values of *XBP1s* mRNAs were normalized to values of total *XBP1* transcripts. (±SD, n=3) ***p<0.0005.

Supplemental Figure. 2. (A) MEF cells were infected with *Toxoplasma* for 18 h and then were incubated with calcium indicator Fluo-4. Fluo-4 intensity is shown as a heat map, with yellow showing the highest Fluo-4 intensity and blue showing the lowest Fluo-4 intensity. (B) WT and *IRE1*$^{-/-}$ cells were transfected with mCherry-ER-KDEL (a marker for the ER) and infected for 18 h with *Toxoplasma*. Cells were then loaded with the low-affinity Ca^{2+} indicator Mag-Fluo-4 AM (green) and the plasma membrane was permeabilized, resulting in Mag-Fluo-4 AM retainment in the ER. Note that the Mag-Fluo-4 AM (green) co-localizes with mCherry-ER-KDEL (red).

Supplemental Figure. 3. (A) WT cells were infected with *Toxoplasma* for 18 h, then fixed with paraformaldehyde and incubated with SAG1 antibody to detect parasites (green); phalloidin shows actin (red) and DAPI shows nuclei (blue). The arrows show lamellipodia at edge of cells. (B) At 18 hpi, infected and uninfected cells were trypsinized and counted, and the same number of cells were used in the transmigration assay. Transmigration was determined by counting the number of cells that transmigrated through membrane. (±SD, n=3), *p<0.05, ***p<0.0005 and

658 ****p<0.0001. ns = not significant. (C) WT and *IRE1*$^{-/-}$ MEF cells were infected using ME49
659 (type II) strain for 18h and transmigration was determined by counting the number of infected
660 cells normalized to noninfected cells (±SD, n=3), ****p<0.0001. (D) WT and ire1 (-) DCs were
661 infected with ME49 strain for 18 h and transmigration was determined by counting the number
662 of infected cells normalized to noninfected cells for 6 h (±SD, n=3), ***p<0.0005.
663
664 **Supplemental Figure. 4.** (A) *IRE1*$^{-/-}$ MEF cells were rescued with WT and mutant versions of
665 transient expression *IRE1* (green), then cells were fixed and stained using KDEL antibody as an
666 ER marker (red); DAPI was used as to visualize nuclei (blue). *Ire1-wt*, *ire1-kD*: kinase domain
667 dead, *ire1-eD*: endoribonuclease dead, *ire1-oD*: *ire1-Δ965* deletion of filamin A binding site
668 [12]. (B) Lysates were prepared from the cells and IRE1, GFP, or actin protein levels were
669 measured by immunoblot analyses using specific antibodies. (C) WT or *IRE1*$^{-/-}$ MEF cells that
670 were rescued with the indicated *IRE1* alleles were cultured in the presence or absence of 1 μM
671 thapsigargin for 6 h and *XBP1s* mRNA levels were measured by RT-qPCR. Values of *XBP1s*
672 mRNA were normalized to total *XBP1* mRNA levels for each condition. (±SD, n=3),
673 ***p<0.0005.
674
675 **Supplemental Figure. 5.** (A) Schematic of IRE1-sgRNAs (1 and 2) and the gene region that was
676 amplified by RT-qPCR to verify loss of *IRE1* expression. (B) Viability assay of DCs at
677 designated hours post-transfection with gRNA-IRE1 (ire1 (-)) or random gRNA (WT). (C)
678 Infected WT and ire1 (-) DCs were incubated with cell tracker and then inoculated into mice by
679 i.p. injection using 10^6 infected cells. At the indicated hpi, the spleen of each mouse was

680 harvested and the cell tracker fluorescence was measured using a plate reader. Values of
681 fluorescence were normalized to uninfected (fold change). **p<0.01 and ****p<0.0001.
682

Fig.1

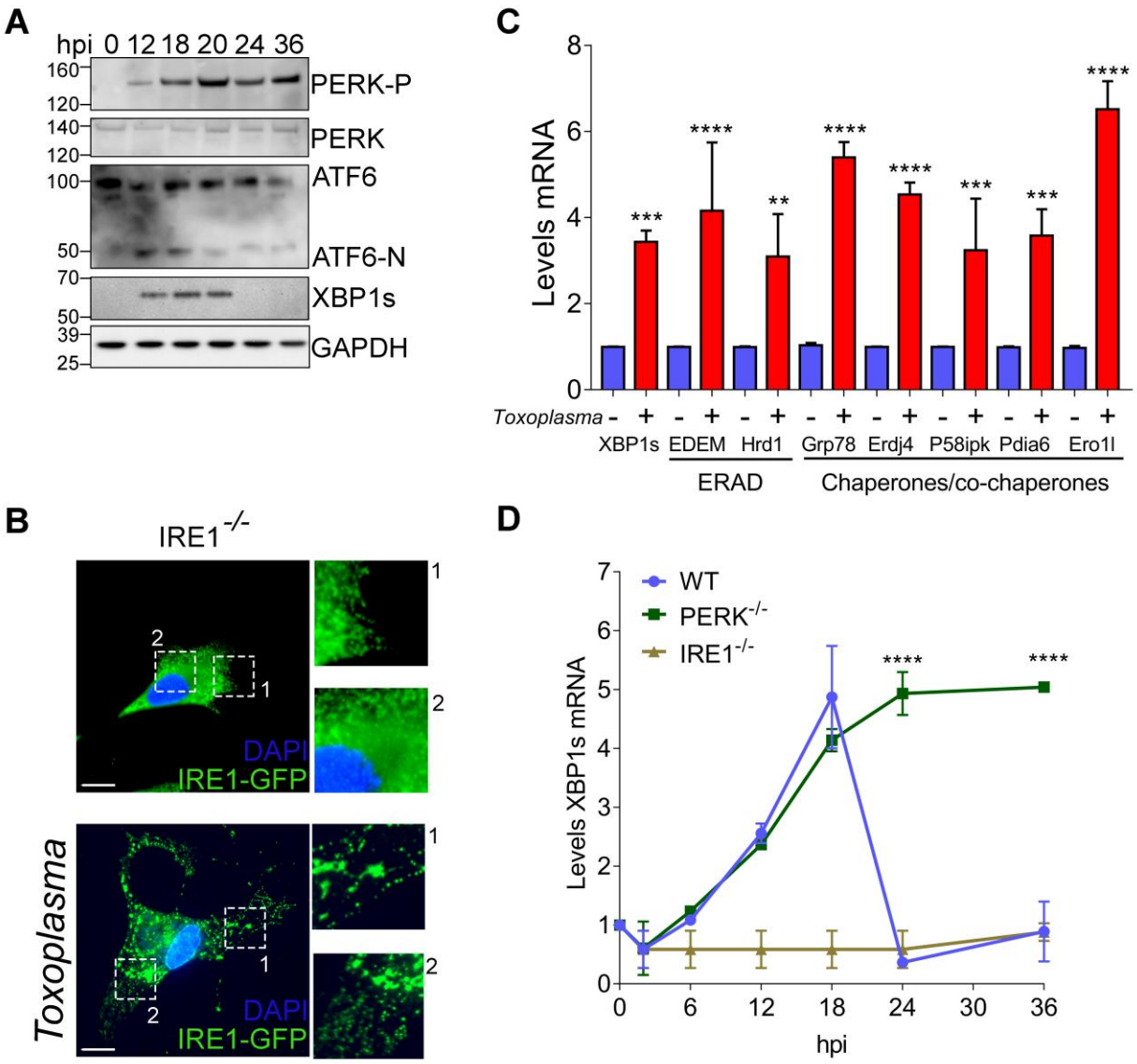

683

684 **Figure. 1. *Toxoplasma* infection triggers activation of the UPR in host cells.** (A) At the
685 indicated times following infection with *Toxoplasma*, cells were harvested and the levels of total
686 PERK, PERK-P, full length ATF6 and ATF6-N, XBP1s, and GAPDH were measured by
687 immunoblot analyses. (B) *IRE1*$^{-/-}$ MEF cells were transfected with a plasmid encoding EGFP-
688 IRE1 (green), followed by infection with *Toxoplasma*. DAPI (blue) was used to visualize host
689 cell and parasites nuclei. Two boxed areas (1 and 2) of each condition are amplified to highlight

690 the IRE1 distribution. Bar=5 µm. (C) MEF cells were infected with *Toxoplasma* for 18 h, or
691 were mock infected, and the mRNA levels of the indicated ERAD/chaperone genes were
692 measured by RT-qPCR. Levels of mRNA were normalized to mock infected, which is
693 represented as a value of 1. (±SD, n=3) ***p<0.001, ****p< 0.0001. (D) *XBP1s* mRNA levels
694 were measured by RT-qPCR at the indicated hpi in WT, *PERK*$^{-/-}$ and *IRE1*$^{-/-}$ MEF cells, as
695 indicated. Levels of *XBP1s* mRNA were normalized to total *XBP1* mRNA in mock infected cells
696 (value of 1) at each time point. (±SD, n=3) ****p<0.0001.
697
698
699
700
701
702
703
704
705
706
707
708
709
710

Fig. 2

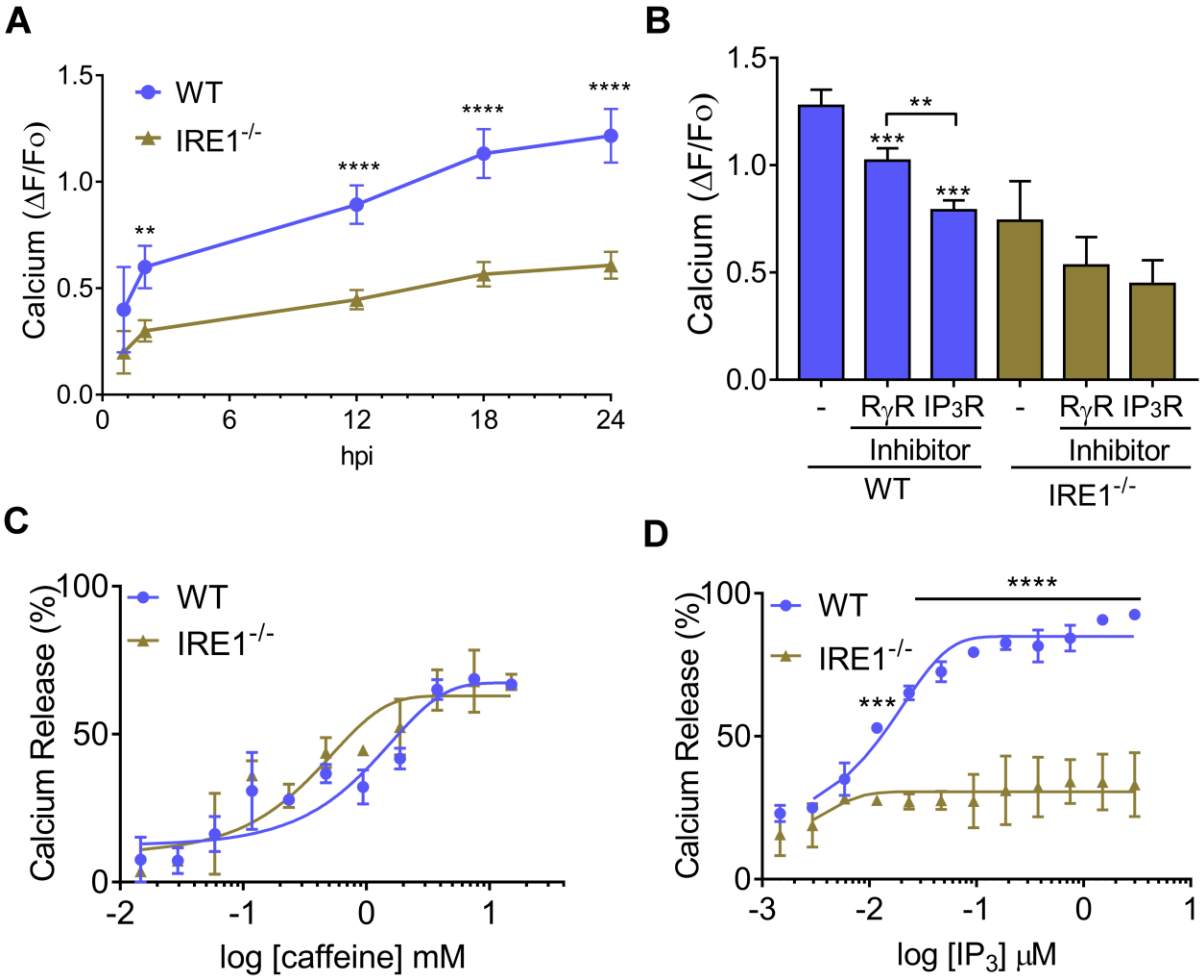

Figure. 2. *Toxoplasma* infection induces calcium release. (A) At the indicated time hpi, cytosolic calcium levels were measured in the infected WT and *IRE1*$^{-/-}$ cells. Values of infected cells were normalized to mock-infected cells (±SD, n=3), **p<0.005 and ****p<0.001. (B) Infected WT and *IRE1*$^{-/-}$ cells were treated with RyR or IP_3R inhibitors for 6 h and the levels of cytosolic calcium were measured. 100 μM Ryanodine (RyR inhibitor) and 0.6 μM Xestospongin C (XeC) (IP_3R inhibitor), (±SD, n=3) **p<0.05, ***p<0.005. Infected cells were incubated with Mag-Fluo-4, followed by plasma membrane permeabilization with saponin and incubation with ATP to maintain the calcium in the ER. To estimate RyR (C) and IP_3R (D) activity, WT and

720 *IRE1*$^{-/-}$ cells infected with *Toxoplasma* for 18 h were treated with caffeine or IP_3 at the indicated
721 concentrations and calcium release is represented the fluorescence using Mag-Fluo-4 as
722 described [19]. Values are represented as the percentage of calcium release and the respective
723 start points were normalized to untreated WT and *IRE1*$^{-/-}$ cells, respectively. (±SD, n=3),
724 **p<0.05, ****p<0.001.
725
726
727
728
729
730
731
732
733
734
735
736
737
738
739
740
741
742

Fig. 3

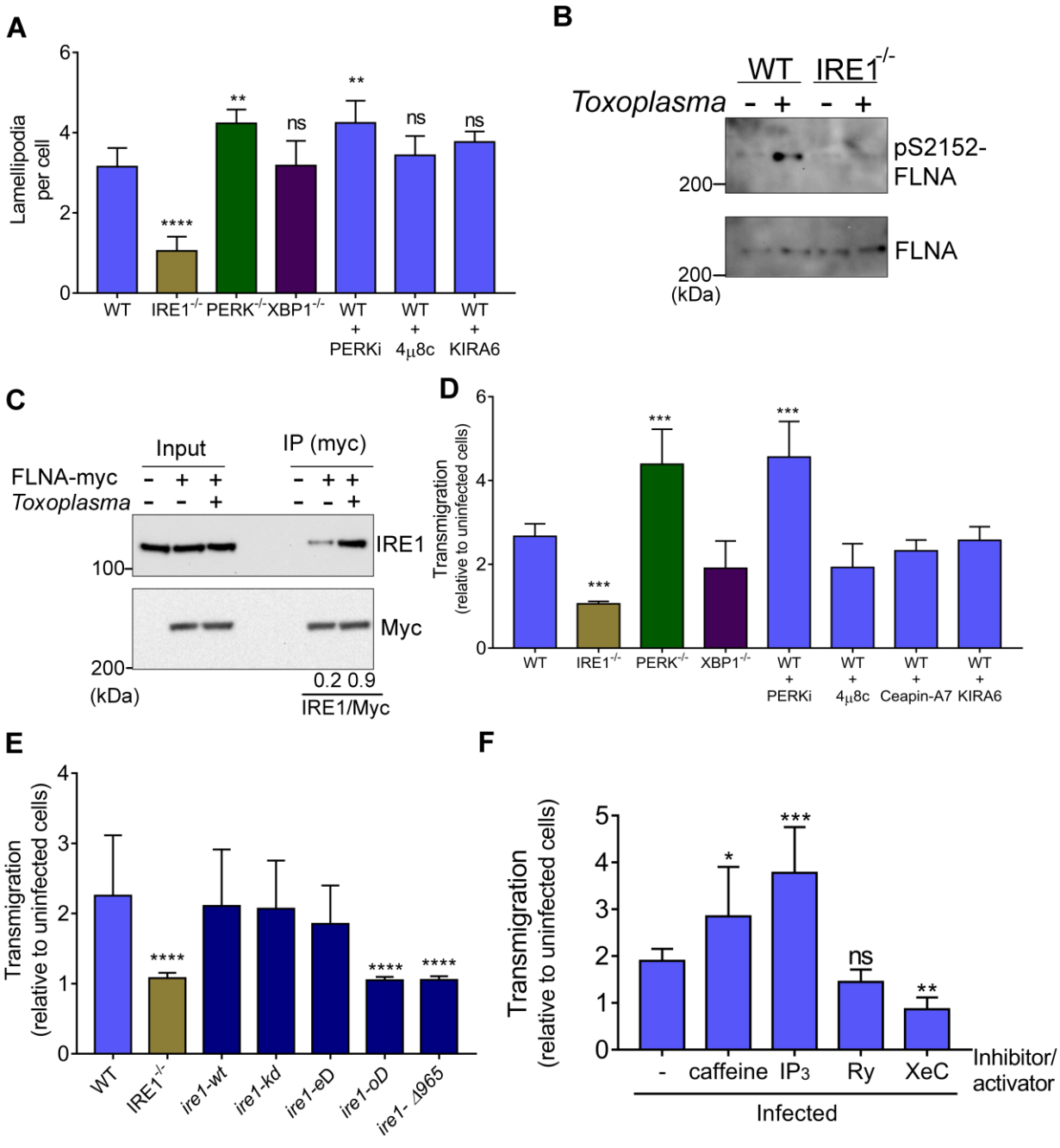

Figure. 3. Activation of IRE1 enhances migration of cells infected with *Toxoplasma*. (A) The numbers of lamellipodia were determined in 50 randomly selected MEF cells infected with *Toxoplasma* 18 hpi and normalized to uninfected cells. Also shown are infected WT cells treated with 1.2 µM PERKi (GSK2656157), 0. 4 µM 4µ8c, 250 nM KIRA6, or 0.2 µM ceapin-A7 for 18

h. (±SD, n=5) **p<0.05, ***p<0.005. (B) WT and *IRE1*$^{-/-}$ cells were infected with *Toxoplasma* for 18 h, then cells were harvested and the levels of filamin A phosphorylation (S2152) were measured by immunoblot analyses. (C) WT cells transiently expressing Myc-filamin A were infected with *Toxoplasma* for 18 h. IP of the tagged Filamin A was carried out using Myc magnetic beads. Bound proteins were separated by SDS-PAGE and the levels of Myc-filamin A and associated IRE1 were measured by immunoblot and compared to uninfected cells. Densitometry of IRE1 signal divided by Myc signal (IRE1/Myc). (D) WT or *IRE1*$^{-/-}$, *PERK*$^{-/-}$, and *XBP1*$^{-/-}$ cells were infected with *Toxoplasma* for 18 h. Alternatively, WT cells were infected with parasite and treated with the following inhibitors during migration per 18 h: 1.2 µM PERKi (GSK2656157), 0.2 µM Ceapin-A7, 250 nM KIRA6, or 0.4 µM 4µ8c. Infected and mock infected cells were trypsinized, counted, and the same number of cells was used for the transmigration assay. Transmigration was determined by counting the number of infected normalized to noninfected cells that migrated through the membrane. (±SD n=3), *** p<0.0005. (E) *IRE1*$^{-/-}$ cells were rescued with *ire1-wt* (wild-type), *kD* (kinase domain-dead- K599A), *eD* (endoribonuclease domain-dead- P830L), *oD* (oligomerization domain-dead- D123P) or *Δ965* (truncated c-terminal *Δ965*), and then a transmigration assay was carried out as described above. (±SD, n=3), ****p<0.0001. (F) Transmigration assay of infected WT MEF cells was carried out in the presence of IP_3R and RyR inhibitors (0.6 µM Xestospongin C, XeC or 100 µM Ryanodine, Ry) or activators (100 µM IP_3 or 1 mM caffeine). (±SD, n=3), *p<0.1, **p<0.05 and ***p<0.0005. ns = not significant.

Fig. 4

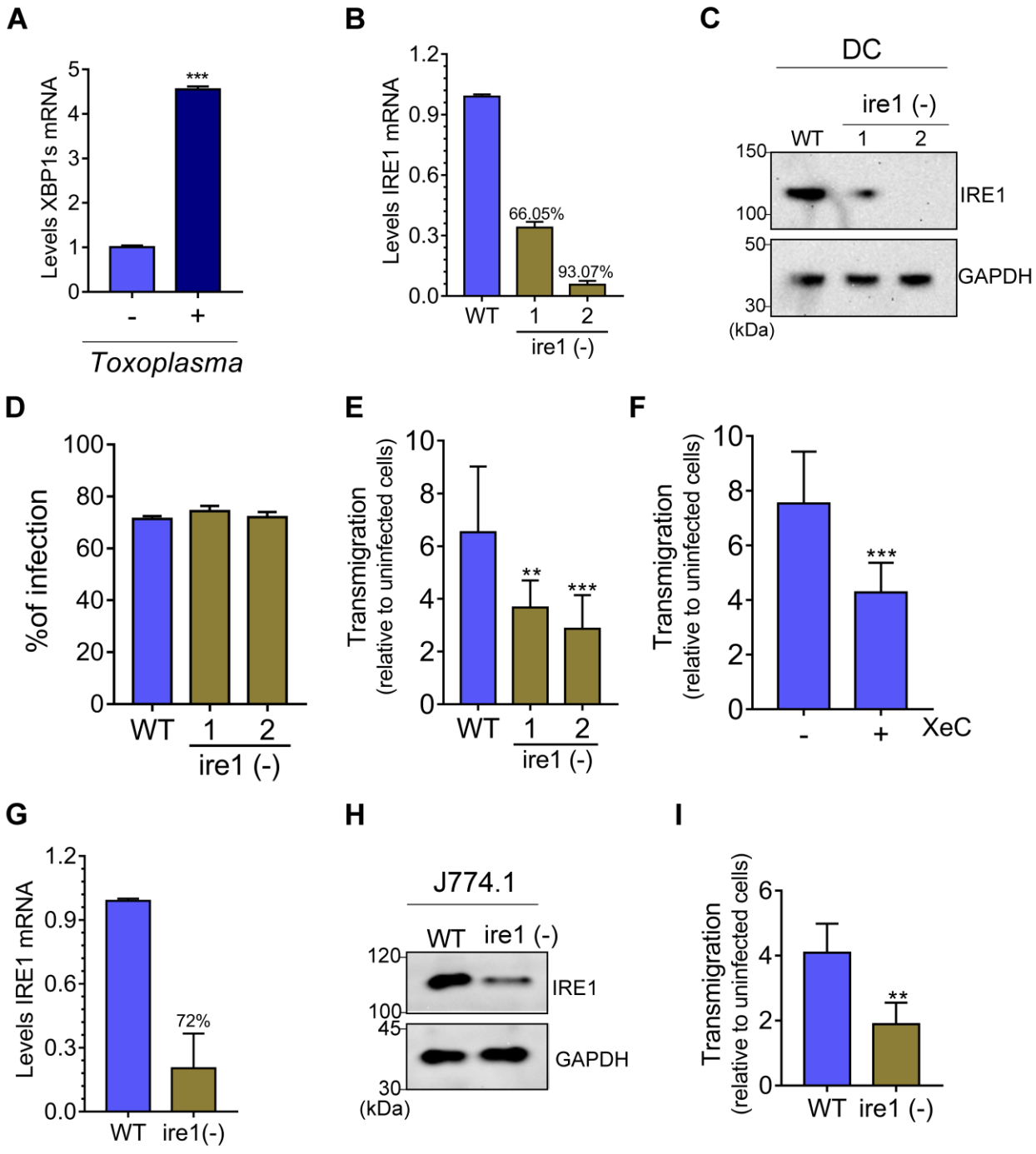

Figure. 4. IRE1 is important for migration of infected DCs. (A) Bone marrow-derived DCs were infected with *Toxoplasma* for 18 h and *XBP1s* mRNA levels were measured by RT-qPCR. The values of XBP1s were normalized to values of total XBP1. (±SD, n=3) ***p<0.0005. (B-C)

The CRISPR/Cas9-engineered depletion of IRE1 in DCs, designated ire (-), was assayed by RT-qPCR and immunoblot using IRE1 antibody compared to WT cells (GAPDH was included as a loading control). (D) Percentage of infection was determined by counting the number of parasites inside 100 WT or ire1 (-) cells. (E) WT and ire1 (-) cells were infected for 18 h and the transmigration assay was carried out for 6 h. Transmigration was determined by counting the number of infected cells normalized to noninfected cells. (±SD, n=3), **$p<0.05$ and ***$p<0.0005$. (F) WT-DCs were infected for 18 h and the transmigration assay was carried out in presence of 0.6 μM xestospongin C (XeC) for 6 h (±SD, n=3), ***$p<0.001$. (G-H) J774.1 macrophages were transfected with sgRNA-2 and the depletion of IRE1 was assayed by RT-qPCR and immunoblot as described in (C). (I) At 18 hpi, WT or ire1 (-) J774.1 macrophages were assayed for transmigration as described above. (±SD, n=3), **$p<0.05$.

Fig.5

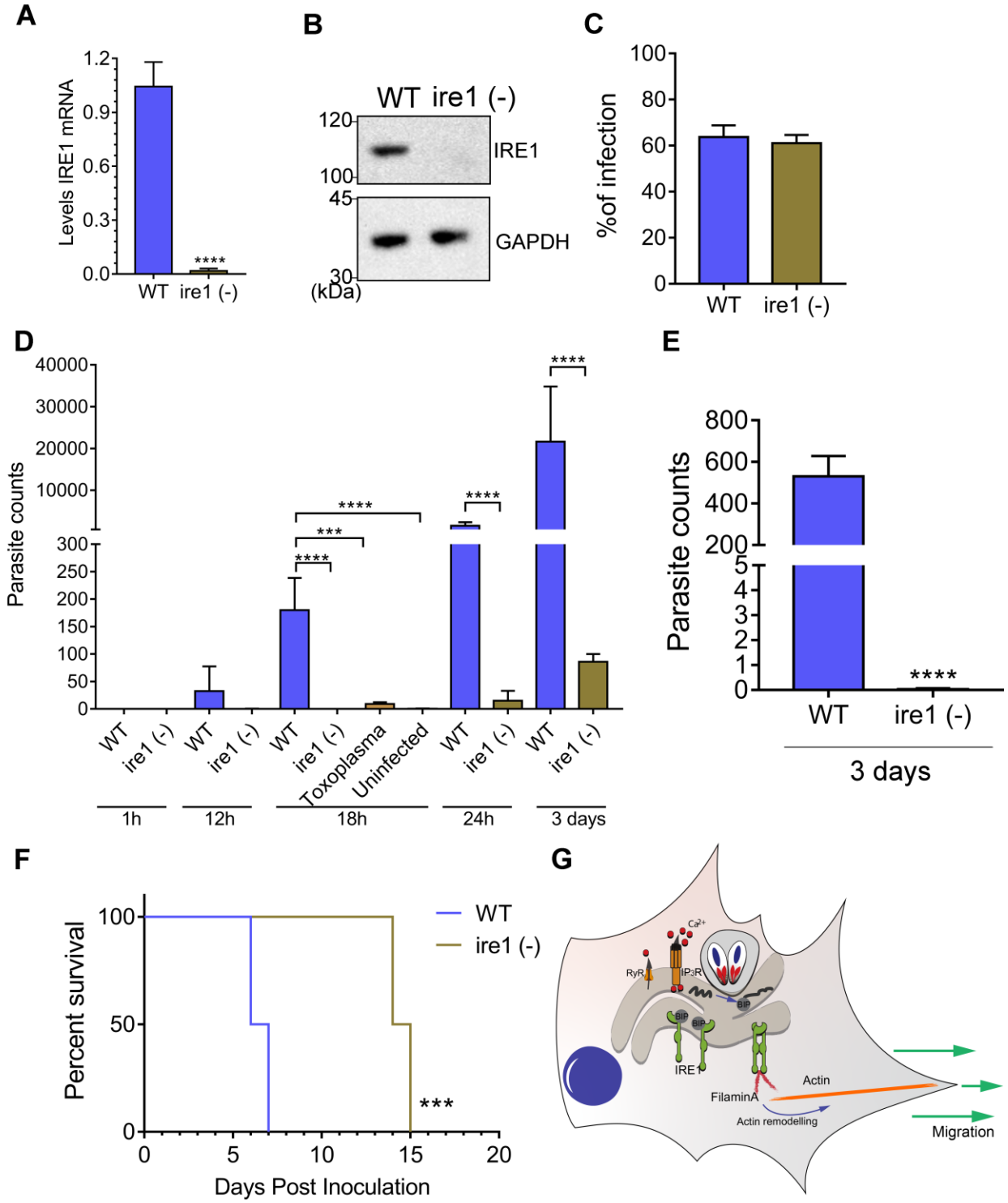

798

799 **Figure. 5. IRE1 facilitates migration of infected DCs *in vivo.*** (A-B) IRE1 was depleted in

800 bone marrow-derived DCs by CRISPR/Cas9 and loss of *IRE1* expression was assayed by RT-

qPCR and immunoblot analyses. (C) WT or ire1 (-) DCs were infected for 18 h and the percentage of infection was determined by counting the number of parasites in 100 cells. (D) Infected WT and ire1 (-) cells were inoculated into mice by i.p. injection (10^6 infected cells). At the indicated hpi, the spleen of each mouse was harvested, and the number of parasites was determined by PCR. ***$p<0.005$ and ****$p<0.0001$. (E) At 3 days post inoculation, the number of parasites was determined in the brain using PCR. ****$p<0.0001$. (F) Survival of C57BL/6 mice challenged with 10^6 infected WT or ire 1 (-) DCs. ***$p<0.0005$. Statistical analyses by Gehan-Breslow-Wilcoxon test. (G) Model for IRE1-direct hypermigration of host cells infected by *Toxoplasma*. During infection, *Toxoplasma* triggers calcium release from the host ER, which creates ER stress and induction of the UPR, which results in enhanced IRE1 association with filamin A. Consequently, the IRE1-filamin A interaction promotes actin remodeling and host cell migration.

Supplemental Fig. 1

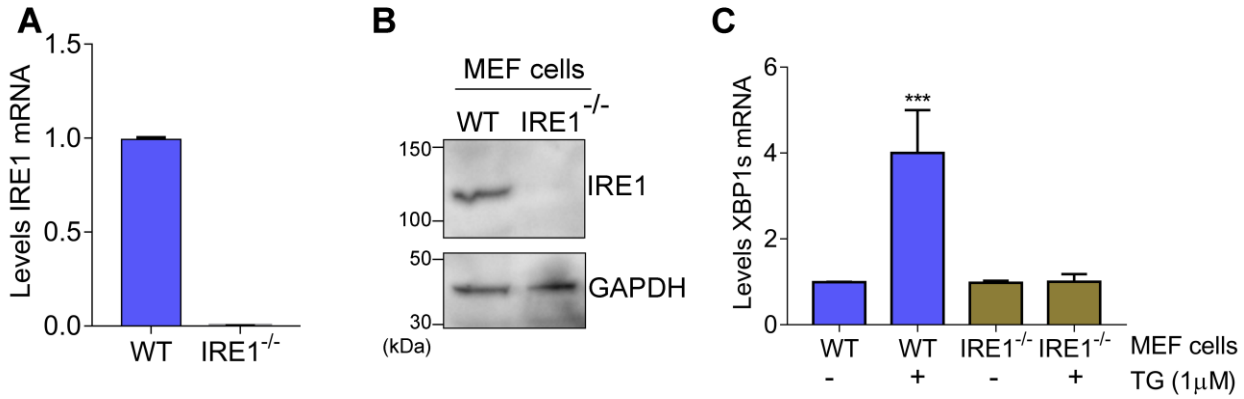

Supplemental Figure. 1. MEF cells were transfected with Cas9 bound to sgRNA targeted to IRE1 as described in the methods section; lowered *IRE1* expression resulting from the CRISPR/Cas9 gene editing was evaluated by (A) RT-qPCR and (B) immunoblot analyses. GAPDH was included as a loading control for the immunoblot analyses. (C) WT and *IRE1*$^{-/-}$ MEF cells were treated with 1 μM thapsigargin (TG), or no stress agent, for 6 h. Cells were then harvested and the *XBP1s* mRNA levels were measured by RT-qPCR. The values of *XBP1s* mRNAs were normalized to values of total *XBP1* transcripts. (±SD, n=3) ***p<0.0005.

Supplemental Fig. 2

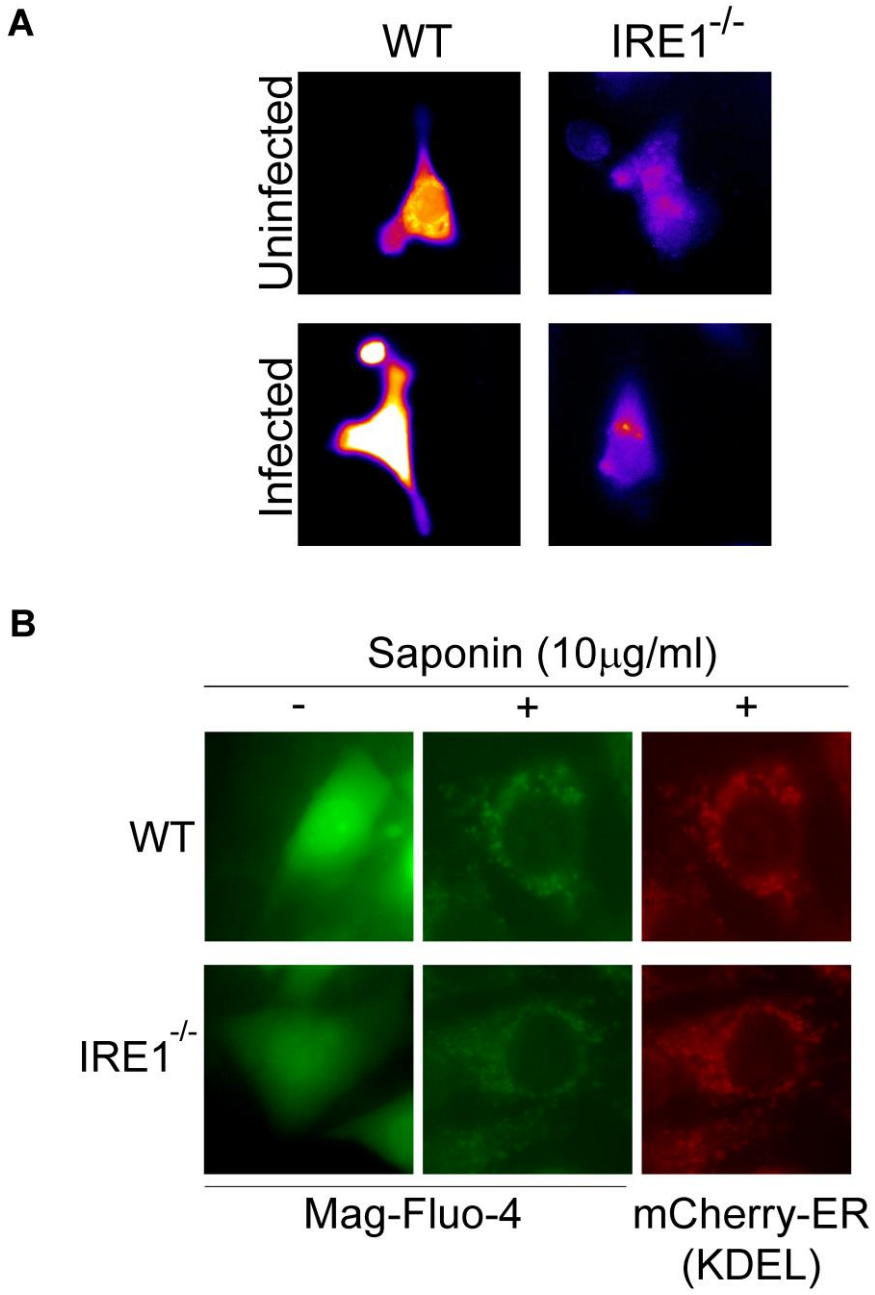

840

841 **Supplemental Figure. 2.** (A) MEF cells were infected with *Toxoplasma* for 18 h and then were

842 incubated with calcium indicator Fluo-4. Fluo-4 intensity is shown as a heat map, with yellow

843 showing the highest Fluo-4 intensity and blue showing the lowest Fluo-4 intensity. (B) WT and

844 *IRE1*$^{-/-}$ cells were transfected with mCherry-ER-KDEL (a marker for the ER) and infected for 18

h with *Toxoplasma*. Cells were then loaded with the low-affinity Ca^{2+} indicator Mag-Fluo-4 AM (green) and the plasma membrane was permeabilized, resulting in Mag-Fluo-4 AM retainment in the ER. Note that the Mag-Fluo-4 AM (green) co-localizes with mCherry-ER-KDEL (red).

Supplemental Fig. 3

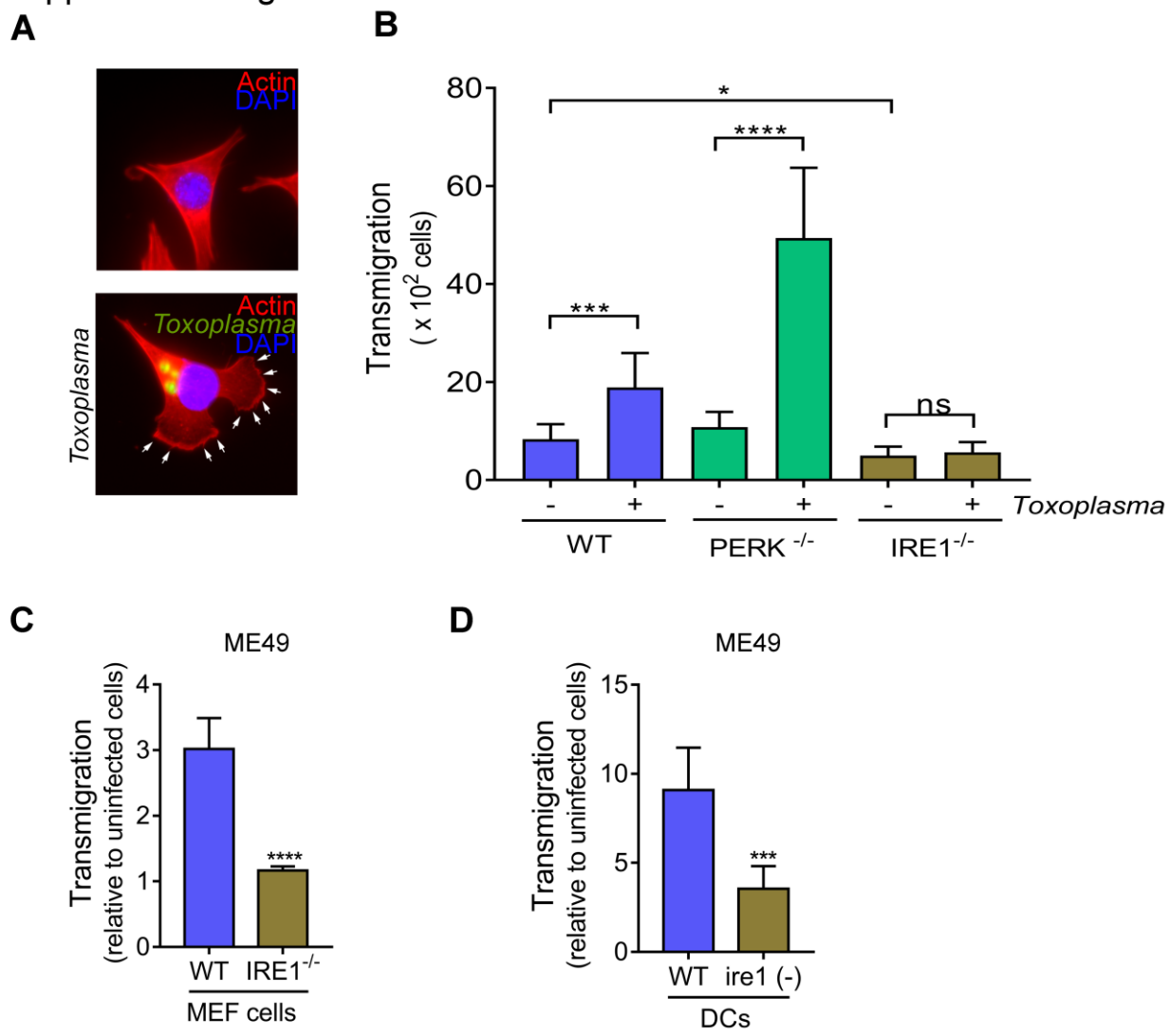

Supplemental Figure. 3. (A) WT cells were infected with *Toxoplasma* for 18 h, then fixed with paraformaldehyde and incubated with SAG1 antibody to detect parasites (green); phalloidin shows actin (red) and DAPI shows nuclei (blue). The arrows show lamellipodia at edge of cells. (B) At 18 hpi, infected and uninfected cells were trypsinized and counted, and the same number of cells were used in the transmigration assay. Transmigration was determined by counting the number of cells that transmigrated through membrane. (±SD, n=3), *p<0.05, ***p<0.0005 and ****p<0.0001. ns = not significant. (C) WT and *IRE1*$^{-/-}$ MEF cells were infected using ME49

(type II) strain for 18h and transmigration was determined by counting the number of infected cells normalized to noninfected cells (±SD, n=3), ****p<0.0001. (D) WT and ire1 (-) DCs were infected with ME49 strain for 18 h and transmigration was determined by counting the number of infected cells normalized to noninfected cells for 6 h (±SD, n=3), ***p<0.0005.

Supplemental Fig. 4

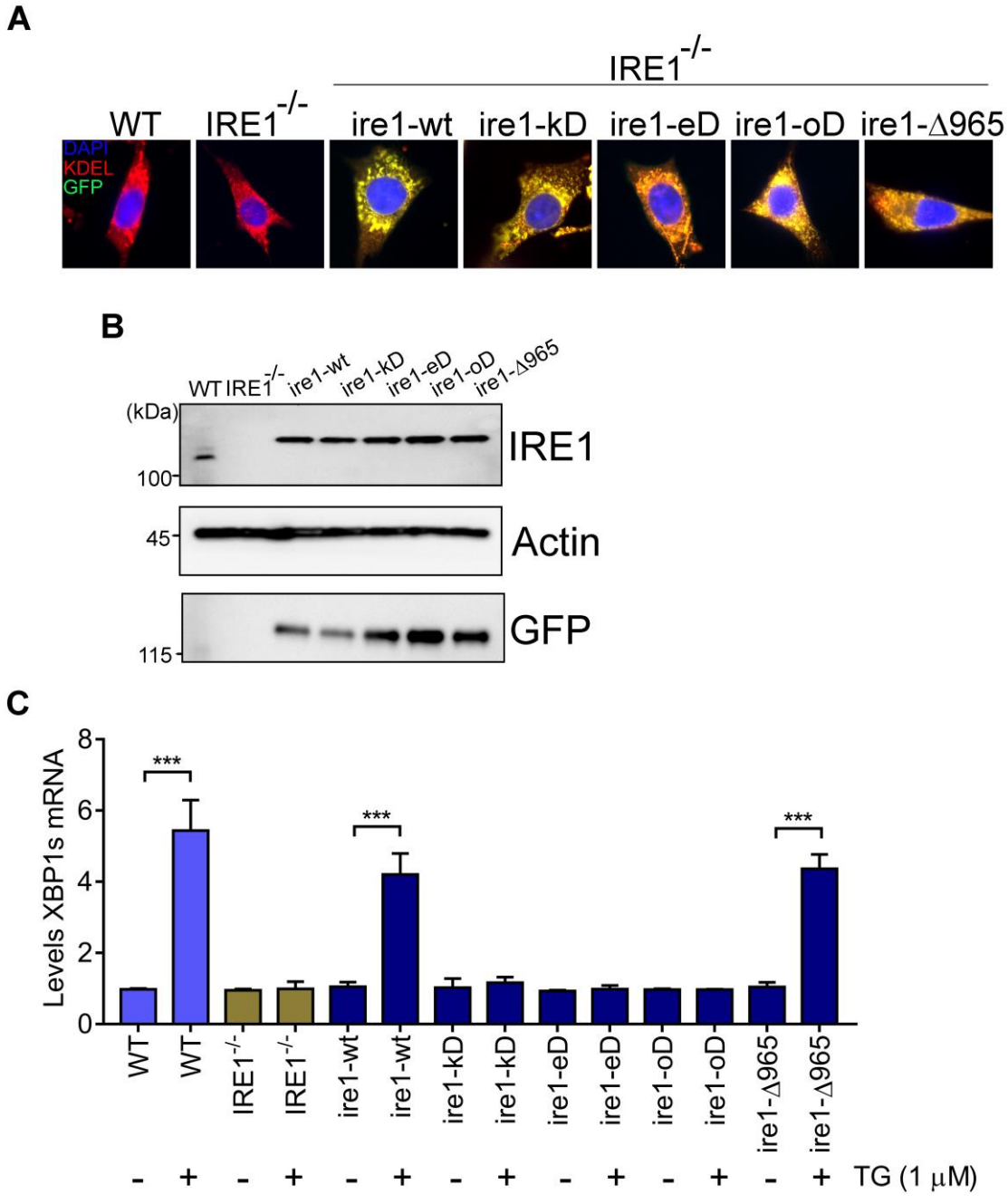

Supplemental Figure. 4. (A) *IRE1*$^{-/-}$ MEF cells were rescued with WT and mutant versions of transient expression *IRE1* (green), then cells were fixed and stained using KDEL antibody as an ER marker (red); DAPI was used as to visualize nuclei (blue). *Ire1-wt*, *ire1-kD*: kinase domain dead, *ire1-eD*: endoribonuclease dead, *ire1-oD*: *ire1-Δ965* deletion of filamin A binding site

[12]. (B) Lysates were prepared from the cells and IRE1, GFP, or actin protein levels were measured by immunoblot analyses using specific antibodies. (C) WT or *IRE1*$^{-/-}$ MEF cells that were rescued with the indicated *IRE1* alleles were cultured in the presence or absence of 1 μM thapsigargin for 6 h and *XBP1s* mRNA levels were measured by RT-qPCR. Values of *XBP1s* mRNA were normalized to total *XBP1* mRNA levels for each condition. (±SD, n=3), ***p<0.0005.

Supplemental Fig. 5

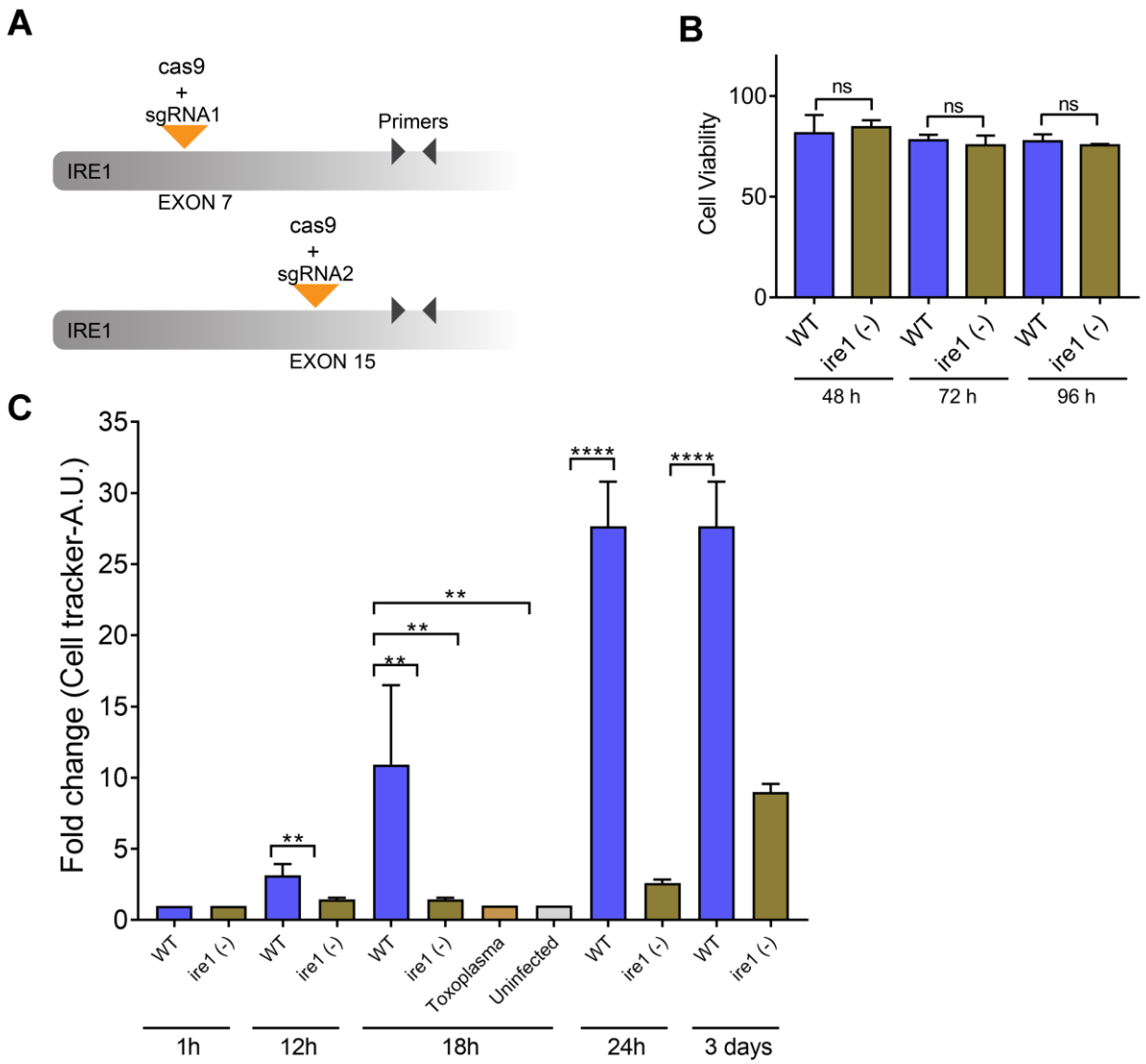

Supplemental Figure. 5. (A) Schematic of IRE1-sgRNAs (1 and 2) and the gene region that was amplified by RT-qPCR to verify loss of *IRE1* expression. (B) Viability assay of DCs at designated hours post-transfection with gRNA-IRE1 (ire1 (-)) or random gRNA (WT). (C) Infected WT and ire1 (-) DCs were incubated with cell tracker and then inoculated into mice by i.p. injection using 10^6 infected cells. At the indicated hpi, the spleen of each mouse was harvested and the cell tracker fluorescence was measured using a plate reader. Values of fluorescence were normalized to uninfected (fold change). **p<0.01 and ****p<0.0001.

929 **Supplementary Table 1 Oligonucleotide primers used in this study.**

Primer	5'—3'
Xbp1-F	ACATCTTCCCATGGACTCTG
Xbp1-R	TAGGTCCTTCTGGGTAGACC
Xbp1u-F	GAAGAGAACCACAAACTCCAGC
Xbp1u-R	GCAGAGGTGCACATAGTCTGAG
Xbp1s-F	GAGTCCGCAGCAGGTG
Xbp1s-R	TCCAGAATGCCCAAAAGG
Edem-F	GGGACCAAGAGGAAAAGTTTG
Edem-R	GAGGTGAGCAGGTCAAATCAA
Hrd1-F	AGCTACTTCAGTGAACCCCACT
Hrd1-R	CTCCTCTACAATGCCCACTGAC
Grp78-F	TGTGGTACCCACCAAGAAGTC
Grp78-R	TTCAGCTGTCACTCGGAGAAT
Erdj4-F	CTTAGGTGTGCCAAAGTCTGC
Erdj4-R	GGCATCCGAGAGTGTTTCATA
P58ipk-F	GTGGCATCCAGATAATTTCCAG
P58ipk-R	GAGTTCCAACTTCTGTGGAAGG
Pdia6-F	TGGTTCCTTTCCTACCATCACT
Pdia6-R	ACTTTCACTGCTGGAAAACTGC
Ero1l-F	CGGACCAAGTTATGAGTTCCA
Ero1l-R	TCAGAGAGATTCTGCCCTTCA
Ire1-wt-F	TCTAGAACCATGCCGGCCCGGCGGCTGCTGCTGCTGCTGAC
Ire1-wt-R	GAGGGCGTCTGGAGTCACTGGGGGCTGGGGCTCTGGGGGCTCG
Ire1-kD-F	GCGACGTGGCCGTGAGGATCCTCCCCGAG
Ire1-kD-R	GGTTGTCAAACATGCCCCGGTACA
Ire1-eD-F	CTCCGAGCCATGAGAGAAGCACCACTACCGGGAGCTGCC

Ire1-eD-R	GAGATCTCTGACAGAACCACCTTTAT
Ire1-oD-F	GGTAAAAAGCAGATCTGGTATGTTATTGACCT
Ire1-oD-R	CATGTAGAGGATTCCATCTGAACTTCGGCATG
Ire1- Δ965-F	TGAGCGAGGGCGGCCCC
Ire1- Δ965-R	CAGCTCCCGGTAGTGGTGCTTCTTATTTC
Gapdh-F	TCACCACCATGGAGAAGGC
Gapdh-R	GCTAAGCAGTTGGTGGTGCA

930

931

Supplementary Table 2 Reagents used in this study.

Reagent	Company names
Antibody	
PERK-P	Phospho-PERK (Thr980) (16F8) Rabbit mAb #3179- Cell Signaling
PERK	PERK (C33E10) Rabbit mAb #3192- Cell Signaling
ATF6	[30]
XBP1s	XBP-1s (D2C1F) Rabbit mAb #12782- Cell Signaling
GAPDH	ab9485-Abcam
Phalloidin	R415-Thermo Fisher Scientific
SAG1	Toxoplasma gondii P30 Monoclonal Antibody (P30/3)- Thermo Fisher Scientific
IRE1	ab37073-Abcam
Myc	Myc-Tag (71D10) Rabbit mAb #2278-Cell Signaling
GFP	clone GFP-20-Sigma Aldrich
Filamin A-P (S2152)	Phospho-Filamin A (Ser2152) Antibody #4761-Cell Signaling
Filamin A	Filamin A Antibody #4762-Cell Signaling
Reagent	
Fluo-4, AM	F14201-Thermo Fisher Scientific
Ry	1329-Tocris
XeC	(-)-Xestospongin C- 1280-Tocris
IP_3	D-myo-Inositol 1,4,5-trisphosphate- 1482-Tocris
caffeine	C53-Sigma Sigma Aldrich
Mag-Fluo-4	M14206- Thermo Fisher Scientific
PERKi	GSK2656157- 5.04651-Sigma Aldrich
4μ8c	4479-Tocris
Ceapin-A7	SML2330-Sigma Aldrich
KIRA6	19151-Cayman Chemical

Collagen I	A1048301-Gibco
Thapsigargin	1138-Tocris
DAPI	D9542-Sigma Aldrich

933